SPRINGER BRIEFS IN APPLIED SCIENCES AND TECHNOLOGY · COMPUTATIONAL MECHANICS

João M. P. Q. Delgado · Eva Barreira
Nuno M. M. Ramos · Vasco Peixoto de Freitas

Hygrothermal Numerical Simulation Tools Applied to Building Physics

Springer

SpringerBriefs in Applied Sciences and Technology

Computational Mechanics

Series Editors

For further volumes:
http://www.springer.com/series/8886

João M. P. Q. Delgado
Eva Barreira · Nuno M. M. Ramos
Vasco Peixoto de Freitas

Hygrothermal Numerical Simulation Tools Applied to Building Physics

Springer

João M. P. Q. Delgado
Eva Barreira
Nuno M. M. Ramos
Vasco Peixoto de Freitas
Faculty of Engineering
Building Physics Laboratory
University of Porto
Porto
Portugal

ISSN 2191-5342 ISSN 2191-5350 (electronic)
ISBN 978-3-642-35002-3 ISBN 978-3-642-35003-0 (eBook)
DOI 10.1007/978-3-642-35003-0
Springer Heidelberg New York Dordrecht London

Library of Congress Control Number: 2012952940

Printed on acid-free paper

Springer is part of Springer Science+Business Media (www.springer.com)

Preface

The subject of this book is to present a critical review on the development and application of hygrothermal analysis methods to simulate the coupled transport processes of Heat, Air, and Moisture (HAM) transfer for one or multidimensional cases.

During the past few decades, there has been quite some development and increased professional use of tools to simulate some of the processes that are involved in the analysis of HAM conditions in individual constructions that form the building envelope or whole building. However, as the vast majority of the hygrothermal models, available in literature, are not readily available to the public outside of the organization where they were developed, in this analysis we only consider the 14 hygrothermal modeling tools that are available to the public in general.

The special features of this book are: (a) a state-of-the-art of numerical simulation tools applied to building physics; (b) the boundary conditions importance; (c) experimental methods for the measurement of relevant material properties, and (d) the numerical investigation and application.

The main benefit of the book is that it discusses all the topics related to numerical simulation tools in building elements and components (including state-of-the-art and applications) and presents some of the most important theoretical and numerical developments in building physics, providing a self-contained major reference that is appealing to both the scientists and the engineers. At the same time, this book will be going to the encounter of a variety of scientific and engineering disciplines, such as civil and mechanical engineering, architecture, etc. The book is divided into several chapters that intend to be a synthesis of the current state of knowledge for benefit of professional colleagues.

The authors would acknowledge with gratitude the support received from the University of Porto-Faculty of Engineering, Portugal, namely the Building Physics Laboratory (LFC). Finally, the authors would welcome reader comments, corrections, and suggestions with the aim of improving any future editions.

João M. P. Q. Delgado
Eva Barreira
Nuno M. M. Ramos
Vasco Peixoto de Freitas

Contents

Symbols

c_p	Heat capacity (J/kg K)
c_{pa}	Heat capacity of air (J/kg K)
c_{pl}	Heat capacity of the liquid water (J/kg K)
c_{pm}	Heat capacity of the solid material (J/kg K)
c_{pp}	Heat capacity of the precipitated salt (J/kg K)
c_{pv}	Heat capacity of water vapor (J/kg K)
D_T	Mass transport coefficient associated with a temperature gradient (m^2/s K)
D_u	Mass transport coefficient associated with a moisture content gradient (m^2/s)
D_w	Liquid moisture diffusivity (m^2/s)
D_φ	Liquid conduction coefficient (kg/ms)
f_l	Liquid fraction having a value from 0 to 1 (−)
g_a	Air flux density (kg/m^2 s)
g_v	Water vapour flux density (kg/m^2s)
h_v	Latent heat of phase change (J/kg)
J_{diff}	Diffusive flux
J_{disp}	Dispersive flux
j_v	Vapour flow (kg/m^2 s)
K	Hydraulic conductivity (kg/ms Pa)
k_w	Water permeability (kg/ms Pa)
L	Length (m)
L_{ice}	Enthalpy of freeze/thaw (J/kg)
L_v	Latent heat of evaporation (J/kg)
p	Vapour pressure (Pa)
p_a	Air pressure (Pa)
P_n	Normal atmospheric pressure (Pa)
p_{sat}	Saturation vapour pressure (Pa)
q_a	Airflow rate (m^3/m^2 s)
Q_h	Heat source volumetric rate (W/m^3)
Q_m	Moisture source volumetric rate (kg/m^3 s)
s	Suction pressure (Pa)
t	Time (s)

T	Temperature (K)
u	Moisture content (kg/kg)
v	Humidity by volume in the surrounding air (kg/m^3)
$\vec{V}_a$	Air velocity vector (m/s)
w	Water content (kg/m^3)

Greek letters

α_s	Absorptivity (−)
δ_a	Vapour permeability in air (kg/ms Pa)
δ_p	Vapour permeability (kg/ms Pa)
δ_v	Vapour permeability (m^2/s)
δ_w	Liquid moisture permeability (kg/ms Pa)
ε	Porosity (m^3/m^3)
θ_g	Volumetric content of the gaseous phase (m^3/m^3)
θ_l	Volumetric content of the liquid phase (m^3/m^3)
θ_p	Volumetric content of precipitated salt (m^3/m^3)
λ	Thermal conductivity (W/m K)
μ	Vapour diffusion resistance factor (−)
μ_a	Air dynamic viscosity (Pas)
ρ	Density of the dry porous material (kg/m^3)
ρ_a	Air partial density (kg/m^3)
ρ_p	Mass density of the precipitated salt (kg/m^3)
ρ_T	Actual total density of the material including moisture contribution (kg/m^3)
ρ_v	Mass density of water vapour (kg/m^3)
ρ_w	Liquid moisture partial density (kg/m^3)
φ	Relative humidity (%)

Chapter 1
Introduction

1.1 Motivation

Building pathologies originated by moisture are frequently responsible for the degradation of building components and can affect users' health and comfort. The solutions for treating moisture related pathologies are complex and, many times, of difficult implementation. Several of these pathologies are due to innovative techniques combined with new materials of poorly predicted performance. The knowledge of the physical processes that define hygrothermal behaviour allows for the prediction of a building response to climatic solicitation and for the selection of envelope solutions that will lead to required feasibility.

Over the last five decades, hundreds of building energy software tools have been developed or enhanced to be used. A list of such tools can be obtained in the US Department of Energy Webpage (2012). This directory provides information for more than 406 building software tools for evaluating energy efficiency, renewable energy and sustainability in buildings.

The problem of moisture damage in buildings has attracted interest from the early days of the last century, but it was during the past decades that the general topic of moisture transport in buildings, became the subject of more systematic study, namely with the development of the modelling hygrothermal performance. In the area of building physics the hygrothermal models are widely used to simulate the coupled transport processes of heat and moisture for one or multidimensional cases. The models may take into account a single component of the building envelope in detail or a multizonal building.

In literature, there are many computer-based tools for the prediction of the hygrothermal performance of buildings. These models vary significantly concerning their mathematical sophistication and, as shown (Straube and Burnett 1991), this sophistication depends on the degree to which the model takes into consideration the following parameters: moisture transfer dimension; type of flow (steady-state, quasi-static or dynamic); quality and availability of information and

J. M. P. Q. Delgado et al., *Hygrothermal Numerical Simulation Tools Applied to Building Physics*, SpringerBriefs in Computational Mechanics,
DOI: 10.1007/978-3-642-35003-0_1, © The Author(s) 2013

stochastic nature of various data (material properties, weather, construction quality, etc.).

All the hygrothermal simulation tools presented later in this paper are based on some numerical methods for space and time discretization. Possible numerical methods are:

- Finite Difference Methods (FDM);
- Finite Control Volume (FCV) methods;
- Finite Element Method (FEM);
- Response Factor;
- Transfer Function method.

The next chapters explore the fundamentals of heat and moisture transfer fundamentals, the relevance of input parameters and different approaches followed, in practice, by available simulation codes. Examples of hygrothermal problems are presented and solved with available tools, demonstrating their potential application.

1.2 Heat and Mass Transfer

The migration of moisture is primarily the result of vapour diffusion and capillary transfer of liquid. Temperature is used as the potential or driving force for heat flow, water vapour pressure is the driving force for the vapour transfer, and capillary suction pressure is the driving force for liquid flow. For a wall assembly, the following equations can be used to represent these three mechanisms for one-dimensional transport:

- For heat conduction (Fourier law)

$$q = -\lambda \frac{\partial T}{\partial x} \tag{1.1}$$

where q is the heat flux (W/m^2), λ is the thermal conductivity of the material (W/m K), T is temperature (K) and x is the length (m).

- For vapour diffusion (Fick's law)

$$n = -\rho D \frac{\partial c}{\partial x} \tag{1.2}$$

where n is the amount of mass flux (mol/m^2 s), ρ is the density (–), D is the diffusion coefficient (m^2/s) and c is the concentration (mol/m^3).

- For capillary transfer (Darcy law)

$$m = -K\frac{\partial P_l}{\partial x} \tag{1.3}$$

where m is the mass flux for liquid water (kg/m^2 s), K is the hydraulic conductivity for liquid (kg/ms Pa) and P_l is capillary pressure (Pa).

The mass balance equation for 1D-transfer and storage of water vapour in a wall with porous building materials, is given by:

$$\frac{\partial w}{\partial t} = \frac{\partial}{\partial x}\left(\delta(\phi)\frac{\partial P}{\partial x}\right) = \rho\zeta(\phi)\frac{\partial}{\partial t}\left(\frac{P}{P_{sat}(T)}\right) \tag{1.4}$$

where δ is the vapour permeability (s), ϕ is the relative humidity (–), w is the moisture content by volume (kg/m^3), $\rho\xi$ is the moisture capacity in terms of relative humidity, derived from the material sorption isotherm (kg/m^3) and $P_{sat}(T)$ is the saturation water vapour pressure at temperature T (Pa). Vapour transfer and storage properties are typically a function of ambient humidity. The boundary condition at the interior material surface is:

$$\delta(\phi)\frac{\partial P}{\partial x}\bigg|_s = \beta_i(P_i - P_s) \tag{1.5}$$

where β_i is the convective surface film coefficient for vapour transfer, P_i is the indoor partial vapour pressure (Pa) and P_s is the vapour pressure at the interior wall surface (Pa).

1.3 Boundary Conditions

1.3.1 Heat Transfer Boundary Conditions

The moisture transport is a strong function of the temperature distribution, which is coupled to heat transfer boundary conditions at the indoor and outdoor surfaces. The boundary condition for the indoor surface results from an energy balance under some simplifying assumptions:

$$-k\frac{\partial T}{\partial y} = (h_{ri} - h_{ci})(T_i - T) + \alpha_{sol}H_{in} + \alpha_{long}H_{eqp} \tag{1.6}$$

where h_{ri} is a linearize indoor radiation coefficient, h_{ci} is the indoor convective heat transfer coefficient, T_i is the indoor temperature, α_{sol} is the absorptance of solar radiation for the wall inner surface, H_{in} is the solar radiation through windows (treated as a source that is evenly distributed to inner surfaces) α_{long} is the absortance for long-wave radiation and H_{eqp} is indoor long-wave radiation caused by equipment, etc.

For the exterior surface, the boundary condition is:

$$-k\frac{\partial T}{\partial y} = h_{co}(T_o - T) + h_{ro}\left(T_{sky} - T\right) + \alpha_{sol}H_{sol} \tag{1.7}$$

where h_{ro} is a linearized outdoor radiation coefficient, h_{co} is the indoor convective heat transfer coefficient, T_o is the ambient air temperature, T_{sky} is the effective sky temperature, α_{sol} is the absorptance for solar radiation and H_{sol} is the incident solar radiation.

1.3.2 Water Vapour Transfer Boundary Conditions

For the indoor and outdoor boundary conditions, the moisture transfer through an air film and finish layer (e.g., paint) is equated to the diffusion transfer into the solid material surface according to:

$$-\mu\frac{\partial P_v}{\partial y} = M_e(P_{va} - P_v) \tag{1.8}$$

where P_v is the water vapour pressure, M_e is the effective mass transfer coefficient and μ is the water vapour permeability.

The effective mass transfer coefficient is the combination of the surface conductance (M_p) and conductance of air film (M_f) associated with convective mass transfer coefficient defined by:

$$M_e = \frac{1}{1/M_f + 1/M_p} = \frac{1}{1/h_m + 1/M_p} \tag{1.9}$$

where h_m is the convective mass transfer coefficient for air in contact with vertical services and it is determined using the Lewis relation (Burch 1995).

1.3.3 Capillary Transfer Boundary Conditions

For the wetted surface condition on the vertical wall it is assumed that there is no liquid flux at the indoor boundary surface. This is also the case for the exterior boundary, when there is no wind-driven rain. However, rain can wet the surface and create a saturated condition. Two conditions are possible:

(a) when the incident rain is insufficient to saturate the surface and all of the available liquid at the surface is transferred into the wall,

$$m_w = K\frac{\partial P_l}{\partial y} \text{ when } K\frac{\partial P_l}{\partial y} \leq m_{rain} \tag{1.10a}$$

(b) the incident rain exceeds the capillary transfer rate limit at the surface condition and the excess is drained from the surface,

$$m_w = m_{rain} \text{ when } K\frac{\partial P_l}{\partial y} \geq m_{rain} \tag{1.10b}$$

where m_w is the mass flux for liquid water and m_{rain} is the mass flux for rain.

References

Burch DM (1995) An analysis of moisture accumulation in the roof cavities of manufactured housing. In: Airflow performance of building envelopes, components, and systems, ASTM STP 1255, American Society of Testing and Materials, Philadelphia, USA, pp 156–177

Straube J, Burnett EFP (1991) Overview of hygrothermal (HAM) analysis methods. In: Trechsel HR (ed) ASTM manual 40-moisture analysis and condensation control in building envelopes, ASTM international, Philadelphia, USA

US Department of Energy Webpage (2012) Building energy software tools directory. Retrieved October 19, 2012, from http://www.eere.energy.gov/buildings/tools_directory

Chapter 2
Inputs for Hygrothermal Simulation Tools

The hygrothermal performance of a construction material can be assessed by analysing energy, moisture, and air balances. The hygrothermal balances consider the normal flows of heat by conduction, convection, and radiation; moisture flows by vapour diffusion, convection, and liquid transport; and airflows driven by natural, external, or mechanical forces.

The prediction of the hygrothermal performance of the building enclosure typically requires some knowledge of geometry of the enclosure, boundary conditions and material properties.

2.1 Geometry of the Enclosure

The enclosure geometry must be modelled before any hygrothermal analysis can begin. In simple methods the geometry is reduced to a series of one-dimensional layers. The enclosure geometry includes all macro building details, enclosure assembly details and micro-details.

2.2 Boundary Conditions

The boundary conditions imposed on a mathematical model are often as critical to its accuracy as the proper modelling of the moisture physics. In general, the following environment needs to be known: Interior environment, exterior environment and boundary conditions between elements.

The correct treatment of the interfacial flows at boundaries between control volumes of different type is an important point in successful modelling.

J. M. P. Q. Delgado et al., *Hygrothermal Numerical Simulation Tools Applied to Building Physics*, SpringerBriefs in Computational Mechanics,
DOI: 10.1007/978-3-642-35003-0_2, © The Author(s) 2013

2.2.1 Exterior Environment

HAM models normally provide hourly evolution of temperature and moisture distributions on the building component under study, considering not only the processes inside the component but also the interaction with the surroundings that, for building physics, is the ambient air (outdoor and indoor). The outdoor ambient air or the exterior environment is described, for most HAM models, in terms of hourly meteorological parameters. The climate data, on hourly bases, that is required for most hygrothermal software tools are:

- Temperature of the exterior air in °C.
- Relative humidity of the exterior air in %.
- Barometric pressure in hPa. This parameter has a small effect on the calculations performed by HAM models, so a mean value over the calculation period may be acceptable.
- Solar radiation incident on the surface in W/m^2. This parameter must include direct and diffuse solar radiation (often reflected solar radiation is neglected). To calculate the total amount of solar radiation incident on the surface, the inclination and the orientation of the surface must be considered. If the HAM models perform these calculations, the climatic data that shall be used is solar radiation (direct and diffuse) on a horizontal surface, which are common meteorological parameters. Otherwise, calculations have to be performed manually or direct measurements must be carried out and then introduced as input data.
- Rain load vertically incident on the exterior surface in l/m^2 h. This parameter, as solar radiation, is not a conventional weather measurement. The determination of this load can be made manually or by the hygrothermal tool. For the calculation it must be considered orientation and inclination of the component and the normal rain in mm, the wind velocity in m/s and the wind direction in °, counted clockwise from north (0°) over east (90°).
- Long-wave atmospheric radiation incident on the surface in W/m^2, if the radiative balance on the surface is to be performed explicitly in the calculation. This parameter may be measured or calculated based on the air temperature, barometric pressure and cloud index. The inclination of the component must be known so the appropriate fraction of the radiation incident on the surface can be calculated from the long-wave atmospheric radiation incident on a horizontal surface.

Common climatic data that is necessary to hygrothermal simulations is: (a) wind velocity [m/s]; (b) wind direction [°] counted clockwise from north (0°) over east (90°); (c) normal rain [mm]; (d) ambient air pressure [hPa]; (e) air temperature [°C]; (f) air relative humidity [%]; (g) direct or global solar radiation incident on a horizontal surface [W/m^2]; (h) diffuse solar radiation incident on a horizontal surface [W/m^2]; (i) thermal radiation of the atmosphere incident on a horizontal surface [W/m^2]; (j) cloud index [–]. This data can be measured by a weather station, can be calculated using weather software tools that create synthetic values

or can result from a statistical treatment of meteorological datasets of individuals months selected from different years over an available data period, containing characteristic weather data of a representative year (Test Reference Years, Design Reference Years, Typical Meteorological Years, etc.).

2.2.2 Interior Environment

The indoor ambient air or the interior environment is characterized by hourly values of temperature, in °C, and relative humidity, in %. These climatic parameters can be provided to the HAM model by a climatic file, containing measured values on the site using temperature and relative humidity probes, or generated values derived from exterior climate. There are a few standards that rule the simulation of indoor climate like EN ISO 13788 (2002), EN 15026 (2007) or ASRAE 160P (2009).

2.2.3 Indoor and Outdoor Surface Transfer

Heat exchanges between the surface and the adjacent air occur by convection. The convective flow is expressed as a function of the convective heat transfer coefficient, h_c (Hagentoft 2001).

$$q_c = h_c \cdot (T_a - T_s) \tag{2.1}$$

The methodology to calculate accurately the convective heat transfer coefficient is not consensual. Different nominal values or functions are available on the literature. The reason for this diversity is the complexity of the convective heat transfer that is dependent on temperature differences between the air and the surface, the magnitude and direction of the air flow and the nature of the surface (geometry and roughness). Table 2.1 presents some examples of functions/values found in the literature for the convective heat transfer coefficient, considering the two types of convection: natural convection, caused by temperature differences, and forced convection, caused by wind, fans, etc.

The radiative heat transfer coefficient, h_r, specifies the long-wave radiation exchange between the building surface and other terrestrial surfaces (sky included), that is governed by the Stefan-Boltzmann Law (σ is the Stefan-Boltzmann constant). As all surrounding surfaces of the building have similar temperatures, the heat flux, q_r, dependent on the fourth power of the temperature, can be linearized with good approximation. Since normally the temperatures of the terrestrial surfaces are not known, they are assumed, by approximation, to be identical to the air temperature.

Table 2.1 Convective heat transfer coefficient

Natural convection		
$h_c = 2 \cdot \lvert T_a - T_s \rvert^{1/4}$	At interior surfaces	Hagentoft (2001)
$0.3 \leq h_c \leq 0.8$	Stable air layers horizontal surface	
$h_c = a \cdot \left(\frac{\Delta\theta}{L}\right)^b$	At ambient temperatures	Hens (2007)
3.5	Inside vertical surfaces	
5.5	Inside horizontal surfaces (heat upwards)	
1.2	Inside horizontal surfaces (heat downwards)	
2.5	Inside vertical surfaces	EN 15026 (2007)
5	Inside horizontal surfaces (heat upwards)	
0.7	Inside horizontal surfaces (heat downwards)	
$3 \leq h_c \leq 10$	–	Kuenzel (1995)
Forced convection		
$h_c = 5 + 4.5 \cdot v_v - 0.14 \cdot v_v^2$	Windward side	Hagentoft (2001)
$h_c = 5 + 1.5 \cdot v_v$	$v_v \leq 10$ m/s	
	Leeward side	
	$v_v \leq 8$ m/s	
$h_c = 5.6 + 3.9 \cdot v_v$	$v_v \leq 5$ m/s	Hens (2007)
$h_c = 7.2 \cdot v_v^{0.78}$	$v_v > 5$ m/s	
19.0	Outside surfaces	
$h_c = 4 + 4 \cdot v_v$	–	EN 15026 (2007)
$h_c = 4.5 + 1.6 \cdot v_v$	Windward side	Kuenzel (1995)
$h_c = 4.5 + 0.33 \cdot v_v$	Leeward side	
$10 \leq h_c \leq 100$	–	

Furthermore, is also assumed that all objects have similar long-wave emissivities, ε, as long as they are non-metallic, which is usually the case in the context of building physics. Three of the four powers of the temperature are lumped together with the radiative heat transfer coefficient and a simple linear relationship analogous to the convective heat transfer is obtained (Hagentoft 2001).

$$q_r = \varepsilon_t \cdot \sigma \cdot T_a^4 - \varepsilon_s \cdot \sigma \cdot T_s^4 \approx h_r \cdot (T_a - T_s) \tag{2.2}$$

$$h_r = 4 \cdot \varepsilon \cdot \sigma \cdot T_0^3 \tag{2.3}$$

where T_0 is an average temperature depending on the surface, the surrounding surfaces and the sky.

Although these temperatures change in time, in most formulations they are assumed as constant. Providing that outside surfaces have similar emissivity, a constant value for the radiative heat transfer coefficient may be adopted. For two close, extended, parallel, plane, non-metallic surfaces more or less at ambient temperature the radiative heat transfer coefficient lies between 3 and 6 W/m^2 K.

Most models consider explicitly the effect of solar radiation as it has an enormous impact on exterior surface temperatures that cannot be included in the radiative heat transfer coefficient. Solar radiation, considered as a source of heat

that increases the surface temperature during the day, depends on short-wave radiation absorptivity, α_s, and on the solar radiation normal to component surface, I_s (Hagentoft 2001)

$$q_s = \alpha_s \cdot I_s \tag{2.4}$$

The solar radiation normal to a surface can be calculated depending on the inclination and orientation of the component, from direct (or global) and diffuse solar radiation incident on a horizontal surface. Short-wave radiation absorptivity depends on the colour and brightness of the material.

Water vapour transfer from air to a surface, or vice versa, is affected by a resistance due to the existence of a boundary air layer. It may be described, in analogy to the heat transfer, by the water vapour transfer coefficient, β_v, and the difference between the vapour pressures of the air, p_v, and of the surface, p_s.

$$g_v = \beta_v \cdot (p_v - p_s) \tag{2.5}$$

The water vapour transfer coefficient depends on the air velocity close to the surface and it can be derived from the convective heat transfer coefficient through some simplifications to the Lewis formula.

$$\beta_v = 7 \cdot 10^{-9} \cdot h_c \tag{2.6}$$

Some numerical HAM models allow simulating the effect of wind-driven rain (WDR) on the water content of a component by introducing a load of moisture on the exterior surface calculated by a semi-empirical model. The semi-empirical models refer to models with a theoretical basis and with coefficients that are determined from measurements. Practically all semi-empirical methods available nowadays are based on the WDR relationship (Eq. 2.7) that estimate the amount of rain that reaches a surface based on the weather data for normal rain, wind velocity and wind direction. One of the biggest problems of these methods is to obtain a reliable WDR coefficient. This value is what distinguishes the models and it can vary between 0.02 and 0.26 s/m (Blocken 2004).

$$R_{WDR} = k \cdot R_h \cdot v \cdot \cos\,\theta \tag{2.7}$$

where R_{WDR} is the wind-driven rain intensity [l/(m^2 h)], k is the WDR coefficient [s/m], R_h is the horizontal rainfall amount [mm/h], v is the wind speed which is admitted to be at 10 m height [m/s], and θ is the angle between the wind direction and the normal to the façade [°].

If the rain load in known and if the surface is not completely wetted the moisture sate of the surface, g_w, can be calculated by Eq. 2.8 (similar to Eq. 2.4 for solar radiation).

$$g_w = \alpha_{WDR} \cdot R_{WDR} \tag{2.8}$$

The concept of precipitation absorptivity, α_{WDR}, allows take into account that a part of the rain water impacting the surface splashes off again. The value of

precipitation absorptivity depends on several factors such as roughness, orientation and nature of precipitation (Kuenzel 1995).

2.3 Material Properties

Hygrothermal simulation is highly demanding on the number of material properties required. Those properties can also present variation with temperature, moisture content and age, as well as present chemical interaction with other materials. Typical material properties needed in hygrothermal simulation include: bulk density, porosity, specific heat capacity, thermal conductivity, vapour permeability, water absorption coefficient, sorption isotherm and moisture retention curve. On the following sections, experimental processes for determination of material properties are described.

2.3.1 Bulk Density (ρ)

Several standards can be applied for the experimental determination of this property, as EN ISO 10545-3 (1995) for ceramic tiles, EN 12390-7 (2000) for concrete, EN 772-13 (2000) for masonry units. The samples must be dried until constant mass is reached. The samples volume is calculated based on the average of three measurements of each dimension.

2.3.2 Porosity (ε)

The standards EN ISO 10545-3 (1995) for ceramic tiles and ASTM C 20 (2000) for fired white ware products, could be used to measure the bulk porosity of building materials. The samples are dried until constant mass is reached (m_1). After a period of stabilization, the samples are kept immersed under constant pressure. Weigh of the immersed sample (m_2) and the emerged sample (m_3) the bulk porosity is given by: $\varepsilon = (m_3 - m_1)/(m_3 - m_2)$.

2.3.3 Specific Heat Capacity (c_p)

This test method employs the classical method of mixtures to cover the determination of mean specific heat of thermal insulating materials. The materials must be essentially homogeneous and composed of matter in the solid state (see ASTM C 351-92b (1999)).

The test procedure provides for a mean temperature of approximately 60 °C (100 to 20 °C; temperature range), using water as the calorimetric fluid. By substituting other calorimetric fluids the temperature range may be changed as desired. All the samples shall be dried to constant mass in an oven at a temperature of 102–120 °C and the method is to add a measured material mass, at high temperature, to a measured water mass at low temperature in order to determine the resulting equilibrium temperature. The heat absorbed by water and container is so calculated and this value equalised to the amount of heat released expression in order to calculate the specific heat desired.

2.3.4 Thermal Conductivity (λ)

The transfer of moisture through common building materials, such as wood, concrete and brick, depends on the complex morphotopological characteristics of the pores in these materials. The thermal conductivity (λ) is a function of temperature and moisture content and is calculated as:

$$\lambda = \lambda_d + C_T\left(T - T_{ref}\right) + C_w w \tag{2.9}$$

where λ_d is the thermal conductivity of the building material under dry conditions and C_T and C_w are temperature and moisture modification coefficients, respectively. The effect of moisture on porous building material properties is quite large (Mendes et al. 2003) and neglecting it can lead to large errors in conduction heat transfer.

The standards ISO 8302 (1991), EN 12664 (2001), EN 12667 (2001) and EN 12939 (2001) can be applied to determine the thermal conductivity of building materials using the Guarded Hot Plate method (Figs. 2.1 and 2.2). The method uses two identical samples of parallel faces that must be dried, prior to the test. After the system stabilization, a constant flux is obtained, perpendicular to the

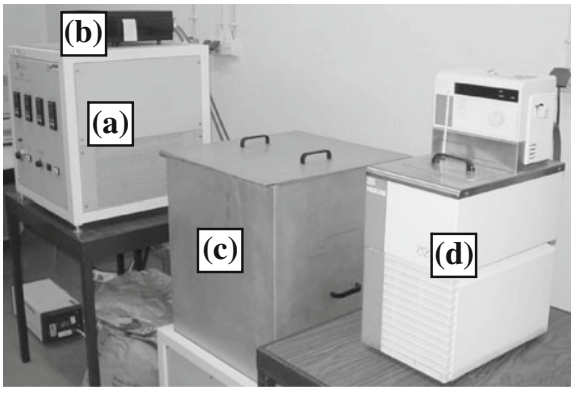

Fig. 2.1 Guarded hot plate device: **a** temperature control, **b** data logger, **c** test vessel, **d** refrigeration equipment

Fig. 2.2 Test vessel containing samples for thermal conductivity measurement

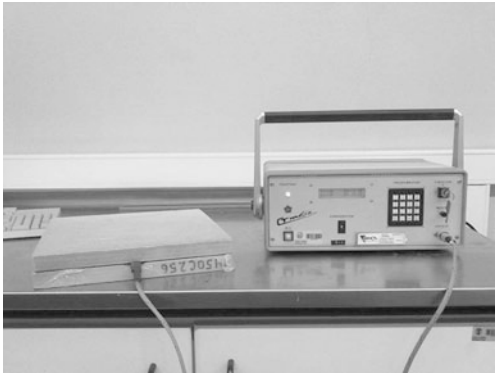

Fig. 2.3 Thermal shock method for determination of thermal conductivity of moist materials

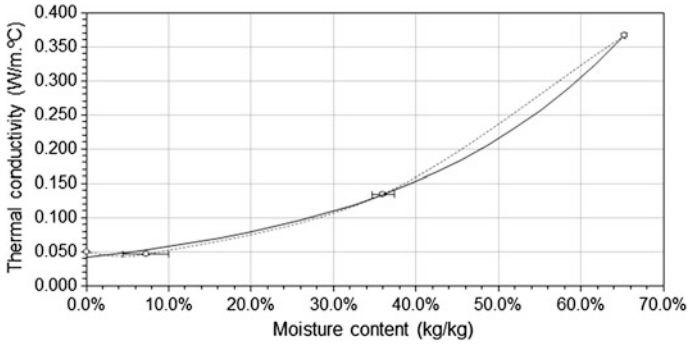

Fig. 2.4 Thermal conductivity variation with moisture content for polyurethane foam

samples dominant faces. Knowing the temperature in opposite faces and the power supply to the hot plate allows determining the thermal conductivity of the samples.

The determination of the thermal conductivity values for moist samples cannot be performed with the guarded hot plate method. The thermal shock method (Fig. 2.3), although less precise, can be used in the characterization of moist materials. The standards EN 993-14 and EN 993-15 describe the method. Figure 2.4 presents a typical variation with moisture content of the thermal conductivity of a thermal insulation product.

2.3.5 Water Vapour Permeability (δ_p)

Vapour permeability is usually determined using the cup test method. The standard EN ISO 12572 (2001) can be used as a reference. The sample is sealed in a cup (Fig. 2.5) containing either a desiccant (dry cup) or a saturated salt solution (wet cup). The set is put inside a climatic chamber (Fig. 2.6) where the relative humidity value is regulated to be different from the one inside the cup. The vapour pressure gradient originates a vapour flux through the sample. The periodic weighing of the cup allows for the calculation of the vapour transmission rate. The method can only be applied if steady-state conditions are achieved through the thickness of the sample. This can be a difficulty for highly permeable materials as the cups will see their initial conditions change very quickly. The test characteristics also imply that it must be performed under isothermal conditions. This can be a difficulty if one intends to reflect the actual behaviour of a material in the envelope. The literature, however, considers that the influence of temperature on the vapour transfer coefficients is negligible.

Figure 2.7 presents an example of vapour permeability test results, using three different materials and three different test conditions. If several values are

Fig. 2.5 Mass determination of a sample sealed in a cup

Fig. 2.6 Cups inside a climatic chamber

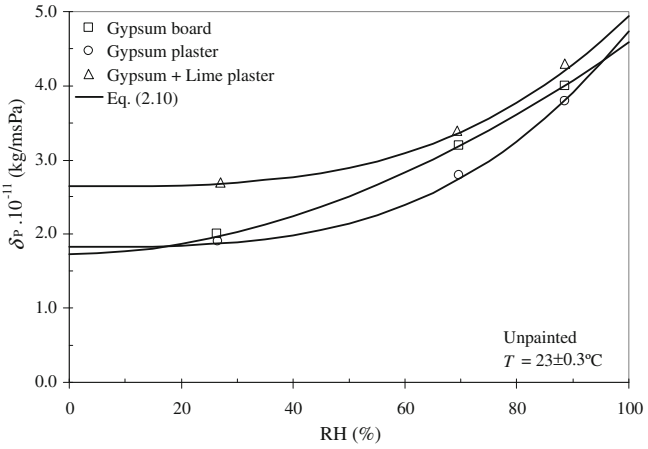

Fig. 2.7 Water vapour permeability for different specimens tested, at 23 °C, and curve fit

available, the points determined in the test a function can be fitted to the results. The literature (see Burch et al. (1992) and Galbraith et al. (1998)) suggests possible functions that typically fit these results. In the example, the following equation was selected:

$$\delta_p(\phi) = A_1 + A_2 \cdot \phi^{A_3} \tag{2.10}$$

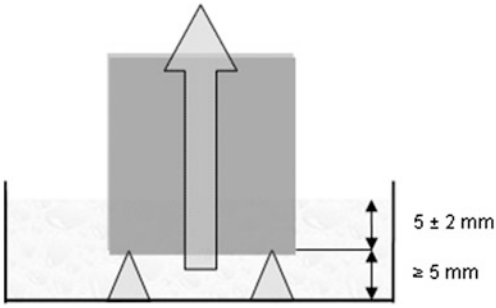

Fig. 2.8 Principle of the water absorption test

2.3.6 Water Absorption Coefficient (A)

The standard EN ISO 15148 (2002) can be applied in the determination of the water absorption coefficient by partial immersion (see Fig. 2.8). The side faces of the samples are made impermeable to obtain a directional flux. After stabilization with the room air, the samples bottom faces are immersed (5 ± 2 mm) and weighed at time intervals defined according to a log scale during the first 24 h period and after that every 24 h. This property is derived from the linear relation between mass variation and the square root of time. When that relation is not verified, only the values registered at 24 h are used.

Liquid transport coefficients can be derived from the water absorption coefficient. As an example, the Eq. (2.11) is used in the WUFI software for estimating liquid diffusivity.

$$D_{\mathrm{ws}}(w) = 3.8\left(\frac{A}{w}\right)^2 1000^{(w-w_f)-1} \tag{2.11}$$

where D_{ws} ($\mathrm{m^2/s}$) is the liquid transport coefficient for suction, A ($\mathrm{kg/m^2\ s^{0.5}}$) is the water absorption coefficient, w ($\mathrm{kg/m^3}$) is the moisture content and w_{f} ($\mathrm{kg/m^3}$) is the free water saturation.

2.3.7 Moisture Storage Functions

The sorption isotherm, describing the moisture storage of a material in the hygroscopic range, can be determined using different methods. Gravimetric type methods are usually preferred for building materials following, for instance, the standard EN ISO 12571 (2000). According to this document, the sorption isotherms are determined by stabilizing material samples in different conditions of relative humidity and constant temperature. The obtained values allow knowing the moisture content of the material at hygroscopic equilibrium with the surrounding air. An apparatus for that test, using salt solutions, can be observed in

Fig. 2.9 Sorption isotherm determination

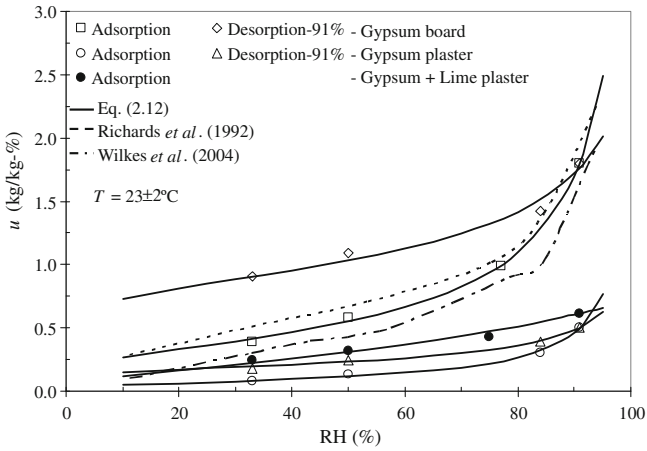

Fig. 2.10 Sorption isotherms for three types of plaster tested and comparison with other results, presented in literature, for the case of gypsum board

Fig. 2.9. In Fig. 2.10 examples of sorption isotherms for gypsum based materials are presented. The difference between adsorption and desorption, hysteresis, is highlighted, as well as the differences that can be found in different sources in literature for what was assumed to be the same material. Equation (2.12) presents an example of a function that is frequently used for fitting sorption test data:

$$u = u_{\mathrm{h}} \cdot (1 - \ln \phi / A_1)^{-1/n} \tag{2.12}$$

Table 2.2 Building material properties

Material	ρ (kg/m^3)	ε (%)	c_p (J/kg K)	λ (W/mK)	A (kg/m^2 s$^{0.5}$)
Stone	1600–2800	0.5–20	1000	0.5–3.5	0.01–0.025
Lime plaster	1600	26	1000	0.8–1.5	0.01–0.25
Concrete	2200	0.18	850	1.6	92
Brick	1000–2400	28	920	0.34–1.04	0.05
Water-repellent final stucco coat	1380	0.36	850	0.87	8
Exterior stucco undercoat	1200	0.3	850	0.25	11
Mineral-bound wood–wool panel	320	0.40	2000	0.09	1.9
Compressed surface of mineral bound wood–wool panel	750	0.15	2000	0.11	10
Medium-density fiberboard (MDF)	255	0.98	2000	0.051	5.0
Mineral wool	60	0.95	850	0.04	1.3
Oriented strand board (OSB)	555	0.6	1880	0.101	287
Liquid vapor retarder coating	1140	0.001	2300	2.3	50000
Gypsum board	1153	0.52	1200	0.32	16
Internal stucco	850	0.65	850	0.20	8.3
Resin finishing coat (acrylic stucco)	2000	0.12	850	0.70	1000
EPS (Expanded polystyrene)	15	0.95	1500	0.04	30
Cement plaster–stucco	2000	0.30	850	1.20	25

The moisture content in the over-hygroscopic region is usually defined using suction curves that can be determined using pressure plate measurements. Since these tests are time consuming, a function is often derived for the moisture storage curve based on a few points determined in sorption tests.

2.3.8 Reference Values

The standards EN ISO 10456 (2007) and EN 12524 (2000) present tabulated design values of hygrothermal properties for a wide range of building materials (see Table 2.2).

References

ASHRAE, 160P (2009) Criteria for moisture control design analysis in buildings. ASHRAE, USA

ASTM, C 20 (2000) Test method for water absorption, bulk density, apparent porosity and apparent specific gravity of fired white ware products. ASTM International, Philadelphia

ASTM, C 351-92b (1999) Test method for mean specific heat of thermal insulation. ASTM International, Philadelphia

Blocken B (2004) Wind-driven rain on buildings—measurements, numerical modelling and applications. PhD thesis, Katholieke Universiteit Leuven, Leuven

Burch DM, Tomas W, Fanney A (1992) Water vapour permeability measurements of common building materials. ASHRAE Trans 98(Part.2):486–494

EN 12390-7 (2000) Testing hardened concrete. Density of hardened concrete. British Standards, London

EN 12524 (2000) Building materials and products—hygrothermal properties—tabulated design values. British Standards, London

EN 12664 (2001) Thermal performance of building materials and products—determination of thermal resistance by means of guarded hot plate and heat flow meter methods—dry and moist products of medium and low thermal resistance. British Standards, London

EN 12667 (2001) Thermal performance of building materials and products—determination of thermal resistance by means of guarded hot plate and heat flow meter methods—products of high and medium thermal resistance. British Standards, London

EN 12939 (2001) Thermal performance of building materials and products—determination of thermal resistance by means of guarded hot plate and heat flow meter methods—thick products of high and medium thermal resistance. British Standards, London

EN 15026 (2007) Hygrothermal performance of building components and elements—assessment of moisture transfer by numerical simulation. British Standards, London

EN 772-13 (2000) Methods of test for masonry units. Determination of net and gross dry density of masonry units (except for natural stone). British Standards, London

EN ISO 10456 (2007) Building materials and products—procedures for determining declared and design thermal values. International Standards Organization, Geneva

EN ISO 10545-3 (1995) Ceramic tiles: determination of water absorption, apparent porosity, apparent relative density and bulk density. International Standards Organization, Geneva

EN ISO 12571 (2000) Hygrothermal performance of building materials and products—determination of hygroscopic sorption properties. International Standards Organization, Geneva

EN ISO 12572 (2001) Hygrothermal performance of building materials and products—determination of water vapour transmission properties. International Standards Organization, Geneva

EN ISO 13788 (2002) Hygrothermal performance of building components and building elements—internal surface temperature to avoid critical surface humidity and interstitial condensation—calculation methods. International Standards Organization, Geneva

EN ISO 15148 (2002) Hygrothermal performance of building materials and products—determination of water absorption coefficient by partial immersion. International Standards Organization, Geneva

EN ISO 8302 (1991) Thermal insulation—determination of steady-state thermal resistance and related properties—guarded hot plate apparatus. International Standards Organization, Geneva

Galbraith G, Mclean R, Guo J (1998) Moisture permeability data presented as a mathematical relationship. Build Res Inf 26(3):157–168

Hagentoft CE (2001) Introduction to building physics. Studentlitteratur, Lund

Hens H (2007) Building physics—heat, air and moisture. Fundamentals and engineering methods with examples and exercises. Ernst & Sohn–Wiley, Belgium

Kuenzel H (1995) Simultaneous heat and moisture transport in building components—one and two dimensional calculation using simple parameters. PhD thesis, IBP Verlag, Stuttgart

Mendes N, Winkelmann FC, Lamberts R, Philippi PC, Mendes N (2003) Moisture effects on conduction loads. Energy Build 35(7):631–644

Richards RF, Burch DM, Thomas WC (1992) Water vapour sorption measurements of common building materials. ASHRAE Trans 98(2):475–485

Wilkes K, Atchley J, Childs P (2004) Effect of drying protocols on measurement of sorption isotherms of gypsum building materials. Performance of Exterior Envelopes of Whole buildings IX International Conference. Clearwater, USA

Chapter 3
Hygrothermal Simulation Tools

Different models for the coupled heat, air, moisture and salt transport have been developed and incorporated into various software programs used in the field of porous building materials and in the closely related field of wetting and drying of soils.

The HAM models (heat, air and moisture) combine the flow equations with the mass and energy balances. Transient, one-dimensional models for combined heat, air and moisture transport in building components have been reasonably well established for about two decades now. In 1996 the final report of Volume 1—Modelling, of the Annex 24 of the International Energy Agency (IEA), elaborated by Hens (1996), showed that 37 programs had been developed by researchers of 12 countries, 26 of which were non-steady sate models. In the last ten years, many programs indicated in this work have developed new versions and improved the conditions of analysis and therefore sensitized the values of results.

In 2003, a review of hygrothermal models for building envelope retrofit analysis made by Canada Mortgage and Housing Corporation (2003) has identified 45 hygrothermal modelling tools, and in the last four years, 12 new hygrothermal models were developed, more of them during Annex 41 (see Table 3.1).

However, most of the 57 hygrothermal models available in literature are not readily available to the public outside of the organization where they were developed. In fact, only the following 14 hygrothermal modelling tools are available to the public in general.

3.1 1D-HAM

The 1D-HAM program is a one-dimensional model for heat, air and moisture transport in a multi-layered porous wall, developed by Lund–Gothenburg Group for Computational Building Physics (1D-HAM webpage: http://www.buildingphysics.com).

J. M. P. Q. Delgado et al., *Hygrothermal Numerical Simulation Tools Applied to Building Physics*, SpringerBriefs in Computational Mechanics,
DOI: 10.1007/978-3-642-35003-0_3, © The Author(s) 2013

Table 3.1 List of hygrothermal models applied in building physics (December 2007)

Model name	Model type	Numerical scheme	Developer
WAND	1D heat-moisture	Steady state Glaser scheme	Catholic University of Leuven, Belgium
KONVEK	3D heat-air-moisture	Steady state	
NATKON	2D heat-air	Steady and non-steady state	
HYGRAN24	1D heat-air-moisture	Non-steady state	
HAM	1D heat-air-moisture	Non-steady state	
HMSOLVER	2D heat-moisture	Non-steady state	
GLASTA	1D heat-moisture	Steady state Glaser scheme	Physibel, Maldegem, Belgium
UMIDUS	1D heat-moisture	Non-steady state	Pontifical Catholic University of Parana, Brazil
PowerDomus	1D heat-moisture	Non-steady state	
HAMPI	1D heat-moisture	Non-steady state	University of Saskatchewan, Canada
WALLDRY	1D heat-air-moisture	Steady state	CMHC, Canada
WALLFEM	1D heat-air-moisture	Non-steady state	
EMPTIED	1D heat-air-moisture	Steady state	
LATENITE	2D heat-moisture	Non-steady state	National Research Council, Canada
hygIRC-1D	1D heat-air-moisture	Non-steady state	
hygIRC-2D	2D heat-air-moisture	Non-steady state	Concordia University, Canada
HAMFitPlus	1/2D heat-air-moisture	Non-steady state	Concordia University, Canada
MATCH	1D heat-air-moisture	Non-steady state	TUD-Thermal Insulation Laboratory, Denmark
BSim2000	1D heat-moisture	Non-steady state	Danish Building Research Institute, Denmark
TRATMO2	2D heat-air-moisture	Non-steady state	VTT-Building Technology, Finland
TCCC2D	2D heat-air-moisture	Non-steady state	
LTMB	1D heat-moisture	Non-steady state	INSA-National Institute of Applied Science, France
CHEoH	2D heat-moisture	Non-steady state	IMF-Institute of Fluid Mechanics, France
TONY	2D heat-moisture	Non-steady state	
V30	1D heat-moisture	Non-steady state	CSTB-Centre for Building Science and Technology, France
V320	2D heat-moisture	Non-steady state	

(continued)

Table 3.1 (continued)

Model name	Model type	Numerical scheme	Developer
SPARK 2.01	1D heat-moisture	Non-steady state	LEPTAB-University of La Rochelle, France
WFTK	1D heat-moisture	Non-steady state	IBP-Fraunhofer Institute for Building Physics, Germany
WUFI-2D	2D heat-moisture	Non-steady state	
WUFI-Plus	1D heat-moisture	Non-steady state	
WUFI-Pro	1D heat-moisture	Non-steady state	
JOKE	1D heat-moisture	Non-steady state	FH-University of Applied Science, Germany
COND	1D heat-moisture	Steady state Glaser scheme	TU-Dresden/FH-Lausitz, Germany
DIM 2.5	2D heat-air-moisture	Non-steady state	TU-Technical University of Dresden, Germany
DELPHIN 5	1/2D heat-air-moisture-pollutant-salt	Non-steady state	
TRNSYS ITT	1D heat-moisture	Non-steady state	
HYGTHERAN	1D heat-moisture	Non-steady state	NBRI- National Building Research Institute, Israel
XAM	1D heat-moisture	Non-steady state	Kinki University, Japan
HYGRO	1D heat-moisture	Steady state Glaser scheme	TNO-Building and Construction Research, Netherlands
WISH-3D	3D heat-air	Steady and non-steady state	
HORSTEN	2D heat-air-moisture	Non-steady state	
HAMLab	1/2/3D heat-air-moisture	Non-steady state	Eindhoven University of Technology, Netherlands
BRECON 2	1D heat-moisture	Steady state Glaser scheme	Building Research Establishment, Scotland
NEV 3	1d heat-moisture	Non-steady state	Slovak Academy of Sciences, Slovakia
NPI	1D heat-moisture	Non-steady state	
PI200A	1D heat-moisture	Non-steady state	SP-Swedish National Testing and Research Institute, Sweden
VADAU	2D heat-moisture	Non-steady state	Chalmers Technical University (Sweden) and Lund University (Sweden) operating as buildingphysics.com in Lund
1D-HAM	1D heat-air-moisture	Non-steady state	
AHCONP ANHCONP	2D heat-air	Steady and non-steady state	
JAM1	1D moisture	Non-steady state	
JAM2	2D moisture	Non-steady state	

(continued)

Table 3.1 (continued)

Model name	Model type	Numerical scheme	Developer
HAM-Tools	1D heat-air-moisture	Non-steady state	Technical University of Denmark/Chalmers Technical University, Sweden
FUNKT 74:6	1D heat-moisture	Non-steady state	Gullfiber AB, Sweden
IDA-ICE	1D heat-air-moisture	Non-steady state	EQUA Simulation AB, Sweden
BMOIST	3D Heat-Moisture	Non-steady state	Purdue University, USA
MOIST	1D heat-moisture	Non-steady state	National Institute for Standards and Testing, USA
FSEC	3D heat-air-moisture- pollutant	Non-steady state	Florida Solar Energy Centre, USA
WUFI-ORNL	1D heat-moisture	Non-steady state	Fraunhofer IBP/Oak Ridge National Laboratory, USA
MOISTURE-EXPERT	1/2D heat-air-moisture	Non-steady state	Oak Ridge National Laboratory, USA

This commercial program uses a finite-difference solution with explicit forward differences in time. Analytical solutions for the coupling between the computational cells for a given air flow through the construction are used. The moisture transfer model accounts for diffusion and convection in vapour phase, but not liquid water transport. Heat transfer occurs by conduction, convection and latent heat effects. Climatic data are supplied through a data file with a maximum resolution of values per hour over the year. The program accounts for surface absorption of solar radiation (Hagentoft and Blomberg 2000).

The governing equations for moisture and energy transfer are, respectively,

$$\frac{\partial w}{\partial t} = -\frac{\partial}{\partial x}\left(\delta_{\mathrm{v}}\frac{\partial v}{\partial x} + q_a v\right) \tag{3.1}$$

$$\rho c_{\mathrm{p}}\frac{\partial T}{\partial t} = -\frac{\partial}{\partial x}\left(\lambda\frac{\partial T}{\partial x} + q_a c_{\mathrm{pa}} T\right) + L_{\mathrm{v}}\frac{\partial w}{\partial t} \tag{3.2}$$

where w (kg/m^3) is the water content of the material, t (s) is the time, δ_{v} (m^2/s) is the vapor diffusion coefficient, q_a (m^3/m^{2}s) is the air flow rate, v (kg/m^3) is the humidity by volume, ρ (kg/m^3) is the density, c_{p} (J/kg K) is the heat capacity, T (K) is the temperature, λ (W/m K) is the thermal conductivity of the wall material, c_{pa} (J/kg K) is the heat capacity of the air and L_{v} (J/kg) is the latent heat of evaporation.

A fictitious surface film is used to account for the surface resistances. The film is simulated as a material layer, fully transparent for solar radiation and with no additional air flow resistance. The surface thermal resistance and the surface vapor resistance for the left and right hand side film layer (without air flow) are given as input.

The transfer of moisture to and from the cells is governed by the humidity by volumes in the cells and the humidity at the boundary. The sorption isotherm is approximated by three straight lines. These should be chosen in order to fit the true sorption isotherm as good as possible. The air flow rate through the structure is the same everywhere. The constant flow resistance together with the pressure difference over the structure determines the air flow rate. The air flow rate can vary in time. The flow resistance can be negative, in order to allow for a changed direction of the air flow.

The input data to the program are supplied through a text file (*.CLI). The climate data i.e. boundary temperatures, solar radiation, humidity by volume, and pressure difference over the wall are given for arbitrary time differences down to hourly values. The boundary values, used in the calculations, are taken as discrete step-wise constant values.

The material properties considered are: the thermal conductivity of the wall material, λ, the density, ρ, the heat capacity, c_{p}, the water content of the material, w, the vapor diffusion coefficient, δ_v and the relative humidity, ϕ.

3.2 BSim

BSim is an integrated PC tool developed by Danish Building Research Institute (SBi) of Aalborg University, for analysing buildings and installations (BSim webpage: http://www.sbi.dk/). It is a one-dimensional model for transport of heat and moisture in porous building materials. The commercial program BSim, the successor of the MATCH program, includes a collection of advanced tools for simulating and calculating e.g. thermal indoor climate, energy consumption, daylight conditions, synchronous simulation of moisture and energy transport in constructions and spaces, calculation of natural ventilation and electrical yield from building integrated photovoltaic systems.

The software can represent a multi-zone building with heat gains, solar radiation through windows, heating, cooling, ventilation and infiltration, steady state moisture balance, condensation risks. A new transient moisture model for the whole building was also developed as an extension of BSim. One of the limitations is that liquid moisture transfer in constructions is not yet represented (Rode and Grau 2004).

The governing equations for moisture and energy transfer are, respectively,

$$\rho \frac{\partial u}{\partial t} = \frac{\partial}{\partial x}\left(\delta_{\mathrm{p}} \frac{\partial p}{\partial x}\right) + \frac{\partial}{\partial x}\left(k_{\mathrm{w}} \frac{\partial s}{\partial x}\right) \tag{3.3}$$

$$\rho c_{\mathrm{p}} \frac{\partial T}{\partial t} = \frac{\partial}{\partial x}\left(\lambda \frac{\partial T}{\partial x}\right) + h_{\mathrm{v}} \frac{\partial}{\partial x}\left(\delta_{\mathrm{p}} \frac{\partial p}{\partial x}\right) \tag{3.4}$$

where ρ is the density of the dry porous material (kg/m^3), δ_p is the vapour permeability (kg/ms Pa), p is the vapour pressure (Pa), k_w is the water permeability (kg/ms Pa), s is the suction pressure (Pa), c_p is the heat capacity (J/kg K), λ is the thermal conductivity (W/m K) and h_v is the latent heat of phase change (J/kg).

When using BSim the building is divided into rooms, some in thermal zones. Only rooms in thermal zones will be simulated dynamically, the rest can be used in other applications. The following groups of information are needed:

- Rooms and thermal zones: The geometry of the rooms are created in the model graphic editor or imported from CAD drawings. Room or rooms are attached to thermal zones by drag and drop in the tree structure of the model.
- Constructions and materials: Description of type, density, thermal capacity, thermal conductivity, and PCM (phase change material) properties. Walls, floors and roof constructions are built in layers according to the description of the materials. All materials and constructions are defined in a database and attached to the model as defaults in one operation or one by one by drag and drop from the database.
- Systems and functions: Internal loads (e.g. persons, lighting, equipment, moisture load), natural single and multi zone ventilation (e.g. infiltration, venting), heating (floor/construction and/or radiator) and cooling radiators, and ventilation systems. All such "systems" are defined by the physical component as well as how it is controlled and when in function.

- Ventilation plants: Supply and exhaust fans as well as total pressure rise and total efficiency. Units of heat recovery, heating and cooling coils, and humidifiers. Together with the control strategy chosen, these data form the base for calculating the power demand and energy consumption necessary for running the ventilation plants.
- Automatic control strategies: Are defined for each individual ventilation plant, e.g. changes in temperature, volume flow, moisture content, readjustment between winter and summer periods. Differentiation is made between data of the physical components of the plant (in the company catalogue) and the control function (automatic or manual equipment).
- Climate data: BSim uses climate data in binary format, but has a built-in function for converting text formatted hourly data to the binary format. This function can automatically convert climate data files in EnergyPlus/ESP-r weather format.

BSim comes with standard libraries for: constructions (walls, floors, roofs, and internal walls), materials, glass, window frames, people loads, schedules and national constants. The connection between the model and the libraries is handled by drag and drop operations in the building model. The user can choose from these libraries or define new input.

3.3 Delphin 5

The Delphin 5 (Webpage: http://bauklimatik-dresden.de) is a commercial program for the analyse of one or two-dimensional model for transport of heat, air, moisture, pollutant and salt transport in porous building materials, assemblies of such materials and building envelopes in general.

The Delphin software can be used in order to simulate transient mass and energy transport processes for arbitrary standard and natural climatic boundary conditions (temperature, relative humidity, driving rain, wind speed, wind direction, short and long-wave radiation).This simulation tools is used for:

- Calculation of thermal bridges including evaluation of hygrothermal problem areas (surface condensation, interstitial condensation);
- Design and evaluation of inside insulation systems;
- Evaluation of ventilated façade systems, ventilated roofs;
- Transient calculation of annual heating energy demand (under consideration of moisture dependent thermal conductivity);
- Drying problems (basements, construction moisture, flood, etc.);
- Calculation of mould growth risks and further applications, etc…

A particular advantage of the numerical simulation program is the possibility of investigation of variants concerning different constructions, different materials and different climates. Constructive details of buildings and building materials can be optimised using the numerical simulation and the reliability of constructions for

different given indoor and outdoor climates can be judged. A large number of variables as moisture contents, air pressures, salt concentrations, temperatures, diffusive and advective fluxes of liquid water, water vapour, air, salt, heat and enthalpy which characterize the hygrothermal state of building constructions, can be obtained as functions of space and time (Nicolai et al. 2007).

The governing equations for moisture mass balance, air mass balance, salt mass balance and internal energy balance are, respectively,

$$\frac{\partial}{\partial t}\left(\rho_{\mathrm{w}}\theta_{\mathrm{l}}+\rho_{\mathrm{v}}\theta_{\mathrm{g}}\right)=-\frac{\partial}{\partial x}\left[\left(\rho_{\mathrm{w}}/v-j_{\mathrm{disp}}-j_{\mathrm{diff}}\right)\theta_{\mathrm{l}}+\left(\rho_{\mathrm{v}}/v+j_{\mathrm{diff}}\right)\theta_{\mathrm{g}}\right] \tag{3.5}$$

$$\frac{\partial}{\partial t}\left(\rho_{\mathrm{a}}\theta_{\mathrm{g}}\right)=-\frac{\partial}{\partial x}\left[\left(\rho_{\mathrm{a}}/v-j_{\mathrm{diff}}\right)\theta_{\mathrm{g}}\right] \tag{3.6}$$

$$\frac{\partial}{\partial t}\left(\rho_{\mathrm{s}}\theta_{\mathrm{l}}+\rho_{\mathrm{p}}\theta_{\mathrm{p}}\right)=-\frac{\partial}{\partial x}\left[\left(\rho_{\mathrm{s}}/v+j_{\mathrm{disp}}+j_{\mathrm{diff}}\right)\theta_{\mathrm{l}}\right] \tag{3.7}$$

$$\begin{aligned}&\frac{\partial}{\partial t}\left[\rho\, c_{\mathrm{p}}T+\rho_{\mathrm{p}}c_{\mathrm{pp}}T\theta_{\mathrm{p}}+\rho_{\mathrm{l}}c_{\mathrm{pl}}T\theta_{\mathrm{l}}+\left(\rho_{\mathrm{v}}c_{\mathrm{pv}}T+\rho_{\mathrm{a}}c_{\mathrm{pa}}T\right)\theta_{\mathrm{g}}\right]\\&\quad=-\frac{\partial}{\partial x}\left[\rho_{\mathrm{l}}c_{\mathrm{pl}}T/v\theta_{\mathrm{l}}+\left(\rho_{\mathrm{v}}c_{\mathrm{pv}}T+\rho_{\mathrm{a}}c_{\mathrm{pa}}T\right)/v\theta_{\mathrm{g}}\right]\\&\qquad-\frac{\partial}{\partial x}\left[-\lambda\frac{\partial T}{\partial x}+\left(h_{\mathrm{s}}-h_{\mathrm{w}}\right)\left(j_{\mathrm{disp}}+j_{\mathrm{diff}}\right)\theta_{\mathrm{l}}+\left(h_{\mathrm{v}}-h_{\mathrm{a}}\right)j_{\mathrm{diff}}\theta_{\mathrm{g}}\right]\end{aligned} \tag{3.8}$$

where ρ_{w} is the liquid moisture partial density (kg/m^3), θ_{l} is the volumetric content of the liquid phase (m^3/m^3), ρ_{v} is the mass density of water vapour (kg/m^3), θ_{g} is the volumetric content of the gaseous phase (m^3/m^3), v is the humidity by volume in the surrounding air (kg/m^3), J_{disp} is the dispersive flux, J_{diff} is the diffusive flux, ρ_{a} is the air partial density (kg/m^3), ρ_{p} is the mass density of the precipitated salt (kg/m^3), ρ_{s} is the mass density of dissolved salt (kg/m^3), θ_{p} is the volumetric content of precipitated salt (m^3/m^3), ρ is the density of the dry porous material (kg/m^3), c_p heat capacity of the solid material (J/kg K), c_{pp} is the heat capacity of the precipitated salt (J/kg K), c_{pl} is the heat capacity of the liquid water (J/kg K), c_{pv} is the heat capacity of water vapour (J/kg K), c_{pa} is the heat capacity of air (J/kg K), λ is the thermal conductivity (W/m K), h_{v} is the partial specific enthalpies of water vapour (J/kg), h_{s} is the partial specific enthalpies of salt (J/kg), h_{w} is the partial specific enthalpies of water (J/kg) and h_{a} is the partial specific enthalpies of air (J/kg).

3.4 EMPTIED

The freeware EMPTIED (webpage: http://www.cmhc-schl.gc.ca/publications/en/rh-pr/tech/1999-123e.html) program is a one-dimensional model for heat, air and moisture transport, with some considerations for air leakage included (Rousseau 1999). The software makes enough simplifying assumptions to be practical for

designers to use in order to compare the relative effects of different climates, indoor conditions, wall materials and air tightness on wall performance. EMPTIED calculates temperatures assuming steady-state conditions for the duration of each bin, neglecting latent heat and heat transported by moving air. The program uses monthly bin temperature data and outputs plots of the monthly amount of condensation, drainage and evaporation. It is recommended for simple analysis of air leakage. EMPTIED has limitations that should be kept in mind. Initial moisture contents cannot be specified. Wind, sun, and rain are not taken into account. Air movement is taken to be the same through every layer, there are no convection loops within layers, or between the exterior and vented cavities. The maximum amount of moisture a material can store safely is assumed to be the same amount at which condensation will start to occur on the surface.

EMPTIED software takes the following information as inputs:

- Month-by-month indoor temperature and humidity conditions. The user can specify them or EMPTIED can calculate them assuming that humidity on the interior comes from ventilation air and normal occupancy, excluding mechanical humidification and unusual occupancies.
- Hourly bin data (counts of the number of hours in an average year that exterior conditions fall into particular combinations of temperature and humidity ranges) for exterior conditions. EMPTIED includes data for several North American cities so the user can select a city.
- Superimposed mechanical pressure or suction, if any (zero is the default).
- Equivalent leakage area per unit area of wall.
- Specifications for layers in the wall, including vapour resistance, maximum capacity for storage of moisture, thermal resistance, and thickness. EMPTIED supplies a menu of common materials with properties already specified, but the user can edit them and add new materials to the list.
- Identification of two layers in the wall where condensation is expected to occur.
- How many years to run the simulation, and what month to start with.

EMPTIED calculates temperatures, assuming steady state conditions for the duration of each bin, neglecting latent heat and heat transported by moving air. Air flows are calculated assuming that the driving force is superimposed pressure plus stack effect pressure over a one storey height (of 2.4 m) due to the temperature difference between interior and exterior for each bin.

Vapour flows are calculated from the resistances specified for materials, the calculated temperatures, and resulting partial pressure of water vapour differences between layers, and between interior and exterior conditions, for each bin.

Condensation is assumed to occur within the specified layers until their storage capacity is exhausted, and then to occur on the surfaces. If condensation during a month exceeds potential evaporation, stored moisture is carried over to the next month. However, moisture condensed on surfaces is assumed to be removed by drainage. Hours below freezing are reported for each layer. All layers are assumed to be dry to start with.

3.5 GLASTA

The commercial program, GLASTA (Webpage: http://www.physibel.be), is a one-dimensional model for heat and moisture transport in porous media. It is based on the Glaser method, but includes a model for capillary distribution within the layers of the assembly and may be suitable for assessing drying potential. The program calculates monthly mean values of temperature and vapour pressure or relative humidity and climatic database for more than 100 European locations are presented (see Physibel 2007).

GLASTA (Physibel 2007) is based on the simple steady-state method of calculation defined in the BS EN ISO 13788:2002 and calculates the temperature, saturation vapour pressure and the vapour pressure in each interface for each period of time as prescribed by the standard. The Glaser method simplifies the physics of moisture and heat transport through the building envelope by assuming the following:

- condensation only occurs at the interface between material layers and remains at that interface;
- thermal conductivity is independent of the moisture content of the material;
- capillary suction and liquid moisture transfer does not occur in the building fabric;
- there is no moisture transfer by convection within the structure of the detail;
- monthly averaged boundary conditions are only used, i.e. the real boundary conditions are not constant over month;
- only one dimensional heat and moisture transfer;
- no solar radiation or driving rain.

3.6 HygIRC

The commercial program hygIRC-1D (webpage: http://www.nrc-cnrc.gc.ca/eng/projects/irc/hygirc.html) it is a one-dimensional simulation tool for modelling heat, air and moisture movement in exterior walls. This program is an advanced hygrothermal model that is an enhanced version of the LATENITE model developed jointly by Institute for Research in Construction and the VTT (Finland). The hygIRC program can be used to model common wall systems. Retrofits to improve the air tightness and insulation levels in the walls were developed and are being applied to the basic wall systems. The hygIRC model will simulate heat, air and moisture conditions within the retrofitted walls to determine how the retrofits affect the durability of the wall system. This information will be used as a means to confirm the integrity of several specific retrofit measures developed for high-rise wall structures before they are recommended to the building industry (Salonvaara and Karagiozis 1994).

The governing equations for moisture, heat, air mass and momentum balance are, respectively,

$$Q_{\mathrm{m}} = \rho \frac{\partial u}{\partial t} + \nabla\left(-\rho D_{\mathrm{w}} \nabla u + \delta_{\mathrm{w}} \rho_{\mathrm{w}} \vec{g} - \delta_{\mathrm{p}} \nabla p + \rho_{\mathrm{v}} \vec{V}_{\mathrm{a}}\right) \tag{3.9}$$

$$Q_{\mathrm{h}} = \frac{\partial(\rho_{\mathrm{T}} c_{\mathrm{P}} T)}{\partial t} + \nabla\left(\rho_{\mathrm{a}} c_{\mathrm{Pa}} \vec{V}_{\mathrm{a}} T\right) - \nabla(\lambda \nabla T) - L_{\mathrm{v}}\left(\nabla(\rho \delta_{\mathrm{p}} \nabla p)\right) + L_{\mathrm{ice}}\left(\rho u \frac{\partial f_{\mathrm{l}}}{\partial t}\right) \tag{3.10}$$

$$\nabla\left(\rho_{\mathrm{a}} \vec{V}_{\mathrm{a}}\right) = 0 \tag{3.11}$$

$$-\nabla p_{\mathrm{a}} + \rho_{\mathrm{a}} \vec{g} - \frac{\mu_{\mathrm{a}}}{k_{\mathrm{a}}} \vec{V}_{\mathrm{a}} = 0 \tag{3.12}$$

where u is moisture content (kg moisture)/(kg dry material), δ_w is the liquid moisture permeability (kg/ms Pa), Q_m is the moisture source volumetric rate (kg/m^{3}s), Q_h is the heat source volumetric rate (W/m^3), p is the vapour moisture pressure (Pa), $\vec{V}_{\mathrm{a}}$ is the air velocity vector (m/s), p_a is the air partial density (kg/m^3), ρ is the density of the dry porous material (kg/m^3), ρ_w is the liquid moisture partial density (kg/m^3), D_w is the liquid moisture diffusivity (m^2/s), δ_p is the vapour water permeability (kg/ms Pa), p_a is the air pressure (Pa), μ_a is the air dynamic viscosity (Pa.s), c_p is the effective specific heat capacity (J/kg K), c_{pa} is the dry-air specific heat capacity (J/kg K), f_l is the liquid fraction having a value from 0 to 1, λ is the effective thermal conductivity (W/m K), L_v is the enthalpy of evaporation/condensation (J/kg), L_{ice} is the enthalpy of freeze/thaw (J/kg) and ρ_T is the actual total density of the material including moisture contribution (kg/m^3).

The hygrothermal modelling tool hygIRC-2D accommodates many advanced features, such as transient heat, air and moisture (liquid and vapour) transport, two-dimensional spatial formulation, variable material properties with moisture content and temperature, air flow through building materials, the effect of solar radiation, the presence of moisture source inside the material, freeze–thaw effect, and many other useful features.

In addition, hygIRC-2D can define accidental moisture entry of any quantity into the wall assembly as a function of time at any location on the wall. This moisture entry function is the final outcome of a laboratory experiment and no detailed runoff and drainage are modelled at present.

To define the construction of the wall system, hyglRC-2D has a pre-processor that allows the user to divide a wall into a number of layers, both in the horizontal and vertical directions. The effective use of this type of advanced numerical tool to analyze and obtain meaningful results, however, demands a proper physical understanding of the problem, an appropriate definition of input parameters and the ability to judiciously interpret the results.

There are a number of major input parameters required for hygIRC-2D simulation, such as: wall construction details, material properties, boundary conditions,

exposure duration, initial moisture content and temperature and accidental moisture entry, quantity and location.

Related to the material properties, the hygIRC-2D requires eight sets of material properties: Air permeability, thermal conductivity, dry density, heat capacity, sorption characteristics, suction pressure, liquid diffusivity and water vapour permeability.

The two main boundary conditions are the outdoor/exterior condition and the indoor/interior condition. The exterior boundary condition is defined by specific weather data and has seven components: temperature, relative humidity, wind velocity, wind direction, radiation (direct, diffused and reflective components), horizontal rainfall and cloud index.

Finally, hygIRC-2D has the capability to inject a certain quantity of moisture that has entered accidentally at any location of the wall and at any time. The quantity of accidentally entered moisture inside the wall and its location were determined from the output of full-scale and small-scale laboratory tests.

3.7 HAMLab

HAMLab is a one-dimensional heat, air and moisture simulation model (Webpage: http://archbps1.campus.tue.nl/bpswiki/index.php/Hamlab). This freeware hygrothermal model is a collection of four tools and functions in the MatLab/Simulink/FemLab environment that includes: HAMBASE (used for: indoor climate design of multizone buildings; energy and (de)humidification simulation; rapid prototyping; and HAM building model component to used with HAMSYS, for the design of HVAC systems), HAMSYS (used for: HVAC equipment design; and controller design), HAMDET (used for: HAM simulation of, up to 3D, building constructions; and airflow simulation in rooms and around buildings) and HAMOP (used for: design parameters optimization; and optimal operation). All tools have been validated, except HAMOP, by comparison with experimental data obtained in the laboratory and in field studies (van Schijndel 2005).

The main objective of HAMBASE is the simulation of the thermal and hygric indoor climate and energy consumption. In SimuLink, the HAMBASE model is visualised by a single block with input and output connections. The interface variables are the input signal of the HAMBASE SimuLink model and the output signal contains for each zone the mean comfort temperature, the mean air temperature and RH. In HAMBASE model the diffusion equations for heat and moisture transfer in the walls are modelled with a finite difference scheme and solved with an implicit method.

3.8 HAM-Tools

HAM-Tools (Webpage: http://www.byggnadsteknologi.se/ibpt.html) is a one-dimensional heat, air and moisture transfer simulation model. The main objective of this freeware tool is to obtain simulations of transfer processes related to building physics, i.e. heat and mass transport in buildings and building components in operating conditions. Using the graphical programming language Simulink and Matlab numerical solvers, the code is developed as a library of predefined calculation procedures (modules) where each supports the calculation of the HAM transfer processes in a building part or an interacting system. Simulation modules are grouped according to their functionality into five sub-systems: Constructions, Zones, Systems, Helpers and Gains (Kalagasidis 2004). The software is an open source, new modules can be easily added by users, and moreover they are free of charge and can be downloaded from the internet. As a disadvantage, some calculations can be slow due to the graphical interface, granularity, complexity, flexibility in modelling.

The governing equations for moisture and energy transfer are, respectively,

$$\frac{\partial w}{\partial t} = -\frac{\partial}{\partial x}\left(K\frac{\partial s}{\partial x} - \delta_{\mathrm{p}}\frac{\partial p}{\partial x} + g_a u\right) \tag{3.13}$$

$$\rho c_{\mathrm{p}}\frac{\partial T}{\partial t} = -\frac{\partial}{\partial x}\left(-\lambda\frac{\partial T}{\partial x} + g_{\mathrm{a}}c_{\mathrm{pa}}T + g_{\mathrm{v}}L_{\mathrm{v}}\right) \tag{3.14}$$

where K is the hydraulic conductivity (kg/ms Pa), s is the suction pressure (Pa), δ_p is the vapour permeability (kg/ms Pa), p is the vapour pressure (Pa), g_{a} is the air flux density (kg/m^{2}s), u is the moisture content (kg/kg), ρ is the density of the dry porous material (kg/m^3), λ is the thermal conductivity (W/m K), c_p is the heat capacity (J/kg K), c_{pa} is the heat capacity of air (J/kg K), g_{v} is the water vapour flux density (kg/m^{2}s) and L_v is the latent heat of evaporation (J/kg)

Using the graphical programming language Simulink® (Matlab), the code is developed as a library of predefined calculation procedures (tools) where each supports the calculation of the HAM transfer processes in a part of a building or in an interacting system. Tools are grouped according to their functionality into five sub-systems: constructions (building envelope parts), zones (air volumes and cavities), systems (HVAC systems), helpers (weather data and basic modelling tools) and gains (casual gains).

When all sub-systems are coupled together and solved simultaneously, the resulting simulation represents the highest level of integration in the HAM-Tools.

In the Simulink graphical approach, the HAM-Tools library appears with the five above mentioned subsystems as separate folders. Representatives of tools or blocks3 from each of the subsystem are shown in the same figure below. Blocks can be modelled separately from each other, with different modelling techniques and with different levels of accuracy.

For the highest level of integration in HAM-Tools, e.g. at the level where a model of a building is assembled, the set of seven signals is used. These are: the surface weather data, the construction array, the system array, the geometry array, the zone array, the radiation array and the gain array.

Finally, the programming capabilities of HAM-Tools are the following:

- 1D calculations of transient heat, air and moisture transfer through a building envelope;
- Transient heat and moisture balances in air zones, assuming well mixed air. At the same time, the mass balance of air can be performed on a multi-zonal grid;
- Coupling between air zones, e.g. multi-zonal calculations;
- Modelling of wind and temperature induced air pressure differences around a building;
- Moisture uptake by surface materials during rain;
- Condensation of surfaces;
- Modelling of the radiation heat exchange with surroundings based on a building orientation.
- Modelling of the radiation heat exchange within air zones based on exact view factors;
- Detailed modelling of internal HAM gains and HVAC equipment;
- Coupling to other codes/procedures developed in Matlab, C++ and Femlab.

And the programme has following the limitations:

- Temperature should be in the range of –30 to 80 °C.
- Effects associated with phase change liquid from/to ice, are neglected.
- Hysteresis is not considered.
- Gravity effects are not considered.
- Chemical reactions are not considered.
- Drainage between material layers is not considered.
- Ageing effects or changes in geometrical dimensions are neglected.

3.9 IDA-ICE 4.5

The commercial program IDA-ICE 4.5 is a numerical tool for building simulation of energy consumption, the indoor air quality and thermal comfort (Webpage: http://www.equa.se). It covers a large range of phenomena, such as the integrated airflow network and thermal models, CO_2 and moisture calculation, and vertical temperature gradients. For example, wind and buoyancy driven airflows through leaks and openings are taken into account via a fully integrated airflow network model. IDA ICE may be used for the most building types for the calculation of:

- The full zone heat and moisture balance, including specific contributions from: sun, occupants, equipment, lighting, ventilation, heating and cooling devices, surface transmissions, air leakage, cold bridges and furniture;
- The solar influx through windows with a full 3D account of the local shading devices and those of surrounding buildings and other objects;
- Air and surface temperatures;
- The operating temperature at multiple arbitrary occupant locations, e.g. in the proximity of hot or cold surfaces. The full non-linear Stephan–Bolzmann radiation with the view factors is used to calculate the radiation exchange between surfaces;
- The directed operating temperature for the estimation of asymmetric comfort conditions;
- Comfort indices, PPD and PMV, at multiple arbitrary occupant locations;
- The daylight level at an arbitrary room location;
- The air, CO_2, and moisture levels, which both can be used for controlling the of VAV (Variable Air Volume) system air flow;
- The air temperature stratification in displacement ventilation systems;
- Wind and buoyancy driven airflows through leaks and openings via a fully integrated airflow network model. This enables one to study temporarily open windows or doors between rooms;
- The airflow, temperature, moisture, CO_2 and the pressure at arbitrary locations of the air-handling and distribution systems;
- The power levels for primary and secondary system components;
- The total energy cost based on time-dependent prices.

To calculate moisture transfer in IDA-ICE, the common wall model RCWall should be replaced with HAMWall, developed by Kurnitski and Vuolle (2000). It can be used either as a single independent model or as a component of a bigger system. HAMWall model is possible to use also as a single program. The moisture transfer is modelled by one moisture-transfer potential, the humidity by volume. The liquid water transport is not modelled and hysteresis is not taken into account. By using this moisture transfer model it is possible to study the following cases:

- The effect of structures on the indoor air quality and thermal comfort;
- The effect of moisture buffering building materials and furniture to dampen the fluctuation of air humidity;
- Making the hygrothermal analysis by taking into account the changes in the indoor climate;
- To study the influence of the ventilation system caused under or over pressure on the hygrothermal conditions in the building envelope;
- To study the influence of moisture on the heating and cooling load and on the performance of heating and cooling equipment.

3.10 MATCH

MATCH (Webpage: http://www.match-box.dk/uk/whatisdatasheet.htm) is a one-dimensional model for heat and moisture transport in composite building structures. A modified version of this commercial program also calculates air flow (Rode 1990). The program uses both the sorption and suction curves to define the moisture storage function and the sorption isotherm in the hygroscopic regime. MATCH uses a Finite Control Volume method to calculate the transient evolution of both the thermal and the moisture related variables, and the moisture transport is assumed to be by vapour flow only, defined by the vapour permeability of the material. In the capillary regime the suction curve is used together with the hydraulic conductivity to model moisture transport. Some applications of the program are:

- determining of the moisture transport in and through building constructions has so far been based on steady state methods which do not consider the hygroscopic capacity of building materials;
- calculating the temperature and moisture profiles transiently by considering the thermal and hygroscopic capacities.

By dividing the time into small steps, it is possible to take into account the effect when constructions are exposed to short, intensive temperature gradients, such as when they are exposed to solar radiation. MATCH, like the similar MOIST, can be used successfully for the approximate analysis and design of protected membrane roofs and walls with non-absorbent cladding. The program has been validated by comparison with experimental data obtained in the laboratory and in field studies.

The governing equations for moisture and energy transfer are, respectively,

$$\rho \frac{\partial u}{\partial t} = \frac{\partial}{\partial x}\left(\delta_{\mathrm{p}} \frac{\partial p}{\partial x}\right) + \frac{\partial}{\partial x}\left(k_{\mathrm{w}} \frac{\partial s}{\partial x}\right) \tag{3.15}$$

$$\rho c_{\mathrm{p}} \frac{\partial T}{\partial t} = \frac{\partial}{\partial x}\left(\lambda \frac{\partial T}{\partial x}\right) + h_{\mathrm{v}} \frac{\partial}{\partial x}\left(\delta_{\mathrm{p}} \frac{\partial p}{\partial x}\right) \tag{3.16}$$

where ρ is the density of the dry porous material (kg/m^3), u is moisture content (kg moisture)/(kg dry material), δ_p is the vapour water permeability (kg/ms Pa), p is the vapour moisture pressure (Pa), k_w is the water permeability (kg/ms Pa), s is the suction pressure (Pa), c_p is the effective specific heat capacity (J/kg K), λ is the thermal conductivity (W/m K) and h_v is the latent heat of phase change (J/kg).

In order to describe the climate in the outdoor surroundings of a construction, a test reference year (TRY) of the particular location is used. A TRY comprises such climatic parameters as temperature, humidity, solar radiation and wind speed. Test reference years, which are available for many locations in Europe and North America, consist of selected, representative periods of actually measured data that have been put together to form a whole year. Alternatively, MATCH may read

files which contain data that represents special kinds of "outdoor climates"—for instance on the external side of a basement wall. Such files may also contain values that have actually been measured.

The indoor climate is described by values of temperature and either a relative humidity or a rate of moisture generation, which are indicated for one month at a time.

MATCH calculates the hygrothermal state of all constructions that are characterized by having a predominant one-dimensional geometry, and where convective transports of heat and moisture have been eliminated. This will typically be constructions like walls and flat and sloped roofs which separate an indoor from an outdoor climate. Employing special climatic data, MATCH may also been used to describe the conditions in other indoor and outdoor constructions.

No moisture calculations are any better than the data being used to describe the transport properties of the materials. MATCH is tied to a data base which contains the thermal and moisture transport characteristics of about 70 materials. The many values for each material are assigned with a simple reference to the name of the material. Thus, the user saves checking with numerous handbooks and tables to have the best material parameters available.

The user interface is made easily accessible by supplying a small preprocessor and by presenting results graphically as the calculations proceed. The intention with MATCH is that it and similar models may one day be regular items in the toolbox of the building designer.

3.11 MOIST 3.0

MOIST 3.0 is a one-dimensional model for heat and moisture transport in building envelopes (Webpage: http://www.bfrl.nist.gov/863/moist.html). This freeware program models moisture transfer by diffusion and capillary flow, and air transfer by including cavities that can be linked to indoor and outdoor air (Burch and Chi 1997). The program enables the user to define a wall, cathedral ceiling, or low-slope roof construction and to investigate the effects of various parameters on the moisture accumulation within layers of the construction as a function of time of year for a selected climate. Much of the material data required by the program are coefficients of curve-fits to specific equations for each property. The equilibrium moisture curves had to be severely approximated, close to the saturation point. Some applications of the MOIST program are:

- predicting the winter moisture content in exterior construction layers;
- predicting the surface relative humidity at the construction layers in hot and humid climates, thereby analysing the potential for mould and mildew growth;
- determining the drying rates for materials containing original construction moisture;
- investigating the performance of cold refrigeration storage rooms;
- analysing the effect of moisture on heat transfer.

Finally, the limitations of the MOIST 3.0 are:

- Wetting of exterior surfaces by rain is not considered;
- Very simple model for coupling of external walls and ambient to internal space:
  (a) does not couple the determination of the indoor air humidity to the moisture transport through exterior structures,
  (b) fully-mixed internal zone state with lumped storage for energy and moisture within internal structures and furnishings (transport of moisture by air movement is neglected),
  (c) neglects the effects of solar transmitted through windows and internal radiative gain,
  (d) doesn't include the effects of wind and ambient temperature on infiltration,
  (e) doesn't consider ground coupling;
- Doesn't consider water pooling around foundation due to groundwater or snow melt;
- Snow insulating effects for horizontal surfaces are neglected;
- Transport of heat by liquid movement in walls is neglected;
- Only considers one-dimensional heat and mass transfer;
- Does not include heat and moisture transfer by air movement (the construction is assumed to be air tight);
- The weather data for European cities are not available and cannot be generated (only have weather data of USA and Canada).

The moisture distribution is governed by the following conservation of mass and energy equations, respectively:

$$\rho \frac{\partial w}{\partial t} = \frac{\partial}{\partial x}\left(\delta_{\mathrm{v}} \frac{\partial p}{\partial x}\right) - \frac{\partial}{\partial x}\left(D_{\varphi} \frac{\partial \varphi}{\partial x}\right) \tag{3.17}$$

$$\rho c_{\mathrm{p}} \frac{\partial T}{\partial t} = \frac{\partial}{\partial x}\left(\lambda \frac{\partial T}{\partial x}\right) + h_{\mathrm{v}} \frac{\partial}{\partial x}\left(\delta_{\mathrm{v}} \frac{\partial p}{\partial x}\right) \tag{3.18}$$

where ρ is the density of the dry porous material (kg/m^3), u is moisture content (kg moisture)/(kg dry material), δ_v is the water vapour permeability (m^2/s), p is the vapour moisture pressure (Pa), D_ϕ is the liquid conduction coefficient (kg/ms), ϕ is the relative humidity (%a), c_p is the effective specific heat capacity (J/kg K), λ is the thermal conductivity (W/m K) and h_v is the latent heat of phase change (J/kg).

3.12 MOISTURE-EXPERT

MOISTURE-EXPERT is a one or two-dimensional model for heat, air and moisture transport in building envelope systems (Karagiozis 2001). This commercial program (Webpage: http://www.ornl.gov) is, basically, software developed by Oak Ridge

National Laboratory and Fraunhofer Institute for Building Physics, to adapt the original European version of WUFI software for USA and Canada. The model treats vapour and liquid transport separately. The moisture transport potentials are vapour pressure and relative humidity, and the energy transport potential is the temperature. The model includes the capability of handling temperature dependent sorption isotherms and liquid transport properties as a function of drying or wetting processes. It is a highly complex program, typically requiring more than 1000 inputs for the one-dimensional simulations. Inputs include: exterior environmental loads, interior environmental loads, material properties and envelope system and subsystem characteristics.

The governing equations for moisture and energy transfer are, respectively:

$$\frac{\partial w}{\partial \varphi}\frac{\partial \varphi}{\partial t} = \nabla\left(D_{\varphi}\nabla\varphi + \delta_{\mathrm{p}}\nabla(\varphi\, p_{\mathrm{sat}})\right) \tag{3.19}$$

$$\frac{\partial H}{\partial T}\frac{\partial T}{\partial t} = \nabla(\lambda\nabla T) + h_{\mathrm{v}}\nabla\left(\delta_{\mathrm{p}}\nabla(\varphi\, p_{\mathrm{sat}})\right) \tag{3.20}$$

where $\partial H/\partial T$ is the heat storage capacity of the moist building material (J/kg), $\partial w/\partial\phi$ is the moisture storage capacity (kg/m^3 %), w is the moisture content (kg/m^3), λ is the thermal conductivity (W/m K), D_ϕ is the liquid conduction coefficient (kg/ms), δ_p is the water vapour permeability (kg/ms Pa), h_v is the evaporation enthalpy of the water (J/kg), p_{sat} is the water vapour saturation pressure (Pa), T is the temperature (K) and ϕ is the relative humidity (%).

3.13 UMIDUS

The freeware program UMIDUS (Webpage: http://www2.pucpr.br/educacao/lst/umidus.html) is a one-dimensional model for heat and moisture transport within porous media, in order to analyze hygrothemal performance of building elements when subjected to any kind of climate conditions (Mendes et al. 1999). Diffusion and capillary regimes are modelled, so moisture transport occurs in the vapour and liquid phases. This freeware model predicts moisture and temperature profiles within multi-layer walls and low-slope roofs for any time step and calculates heat and mass transfer.

Input files containing hourly data provide information on the conditions at the interior and exterior of the wall. A library of material properties is also available. The orientation and tilt of the wall are considered and convection heat transfer coefficients at the exterior of the wall are calculated hourly from wind velocity data. The program needs to be validated.

The governing equations for mass and energy transfer are, respectively,

$$\frac{\partial u}{\partial t} = -\frac{\partial}{\partial x}\left(-D_{\mathrm{T}}\frac{\partial T}{\partial x} - D_{\mathrm{u}}\frac{\partial u}{\partial x}\right) \tag{3.21}$$

Table 3.2 Some information of the 14 hygrothermal models available to the public in general

Name	Material properties														Boundary conditions (outside)										Boundary conditions (inside)			
	1	2	3	4	5	6	7	8	9	10	11	12	13	14	A	B	C	D	E	F	G	H	I	J	a	b	c	d
1D-HAM	X		X	X	X	X							X		X	X	X	X				X			X	X		
BSim2000	X	X	X	X	X	X						X		X	X	X	X	X	X	X		X	X		X	X	X	
Delphin 5	X	X	X	X	X		X	X	X		X		X		X	X	X	X	X	X	X	X			X	X	X	
EMPTIED	X		X	X		X		X					X		X	X	X								X	X	X	
GLASTA	X		X	X		X	X								X	X		X				X			X			
hygIRC-1D	X		X	X	X	X		X	X				X		X	X		X	X	X	X		X	X	X	X			X
HAMLab	X		X	X			X			X		X			X	X			X	X		X	X		X	X		
HAM-Tools	X	X	X	X	X	X		X			X		X		X	X	X	X	X	X	X	X	X		X	X	X	
IDA-ICE[a]	X		X	X	X	X						X	X		X	X	X	X	X	X		X			X	X		
MATCH	X	X	X	X	X	X		X			X	X		X	X	X		X	X		X	X	X		X	X		
MOIST	X		X	X	X	X		X	X				X		X	X		X	X	X			X		X	X		
MOIST-EXP.	X	X	X	X	X	X		X	X		X	X	X		X	X	X	X	X	X	X	X	X	X	X	X	X	
UMIDUS	X	X	X	X	X		X								X	X		X	X	X					X	X		
WUFI[b]	X	X	X	X	X	X			X	X	X	X			X	X		X	X	X	X	X	X		X	X		

[a] IDA-ICE version with HAMWall;

[b] WUFI family: WUFI-Plus, WUFI-2D, WUFI-Pro and WUFI-ORNL/IBP. A free research and education version of WUFI-ORNL/IBP for USA and Canada is available

$$\rho c_{\mathrm{p}} \frac{\partial T}{\partial t} = \frac{\partial}{\partial x}\left(\lambda \frac{\partial T}{\partial x}\right) + h_{\mathrm{v}} \frac{\partial}{\partial x}\left(D_{Tv}\rho_l \frac{\partial T}{\partial x} + D_{uv}\rho_l \frac{\partial u}{\partial x}\right) \tag{3.22}$$

where u is moisture content (kg moisture)/(kg dry material), D_T is the mass (liquid + vapour) transport coefficient associated with a temperature gradient (m^2/sK), D_u is the mass (liquid + vapour) transport coefficient associated with a moisture content gradient (m^2/s), ρ is the density of the dry porous material (kg/m^3), c_p is the effective specific heat capacity (J/kg K), λ is the thermal conductivity (W/m K), h_v is the latent heat of phase change (J/kg), D_{Tv} is the vapour phase transport coefficient associated with a temperature gradient (m^2/s K), D_{uv} is the vapour phase transport coefficient associated with a moisture content gradient (m^2/s) and ρ_l is the liquid mass density (kg/m^3).

The model does not take into account the gravity influence on the transfer of liquid water through roofs. Related to boundary conditions adopted by UMIDUS software, the outside surface of the wall is exposed to solar radiation, heat and mass convection, and phase change. Internally, the wall is exposed to heat and mass convection and phase change.

In order to reduce CPU time and in the case there is a lacking of data, the program presents 6 sub-models derived from Eq. (3.22). The authors related the "apparent" thermal conductivity, λ_{app}, with the "pure" thermal conductivity, λ, by the following expression:

$$\lambda_{app} = \lambda + h_{\mathrm{v}} D_{Tv} \rho_l \tag{3.23}$$

The 6 sub-models are:

- Submodel 0: This model is the same as the original model given by Eqs. (3.21) and (3.22).
- Submodel 1: This model is the same as the original model except that all coefficients are taken to be constant.
- Submodel 2: This model omits the source term in Eq. (3.22), which is associated with a moisture gradient, resulting:

$$\rho c_{\mathrm{p}} \frac{\partial T}{\partial t} = \frac{\partial}{\partial x}\left(\lambda_{app} \frac{\partial T}{\partial x}\right) \tag{3.24}$$

- Submodel 3: This model is obtained disregard the term: $h_{\mathrm{v}} D_{Tv} \rho_l$, resulting:

$$\rho c_{\mathrm{p}} \frac{\partial T}{\partial t} = \frac{\partial}{\partial x}\left(\lambda \frac{\partial T}{\partial x}\right) \tag{3.25}$$

- Submodel 4: This model is the same as Submodel 3, except that the pure thermal conductivity, λ, is constant.
- Submodel 5: This model takes the coefficients D_{u}, D_{T} and λ to be constant.

The UMIDUS submodel 0 is the most precise, therefore the most time consuming model. Submodel 5 is the simplest and fastest heat and mass transfer model. Submodel 4 is equivalent to the model employed in MOIST program version 2.

The UMIDUS submodels are solved with a finite-volume approach that uses a fully implicit solution scheme with coupling between the conservation equations.

3.14 WUFI

WUFI family, a commercial program, is a one or two-dimensional model for heat and moisture transport developed by Fraunhofer Institute in Building Physics (Webpage: http://www.wufi-pro.com). It is validated using data derived from outdoor and laboratory tests, allows realistic calculation of the transient hygrothermal behaviour of multi-layer building components exposed to natural climate conditions (Kuenzel and Kiessl 1997; Kuenzel 1995). Heat transfer occurs by conduction, enthalpy flow (including phase change), short-wave solar radiation and long-wave radiative cooling (at night). Convective heat and mass transfer is not modelled. Vapour-phase transport is by vapour diffusion and solution diffusion, and liquid-phase water transport is by capillary and surface diffusion.

The governing equations for moisture and energy transfer are, respectively,

$$\frac{\partial w}{\partial \varphi}\frac{\partial \varphi}{\partial t} = \nabla\left(D_{\varphi}\nabla\varphi + \delta_{\mathrm{p}}\nabla(\varphi\, p_{\mathrm{sat}})\right) \tag{3.26}$$

$$\frac{\partial H}{\partial T}\frac{\partial T}{\partial t} = \nabla(\lambda\nabla T) + h_{\mathrm{v}}\nabla\left(\delta_{\mathrm{p}}\nabla(\varphi\, p_{\mathrm{sat}})\right) \tag{3.27}$$

and the water vapour diffusion resistance factor, μ, used by WUFI is given by,

$$\mu = \frac{\delta_{\mathrm{a}}}{\delta_{\mathrm{p}}} = \frac{2.0 \times 10^{-7} T^{0.81}/P_{\mathrm{n}}}{\delta_{\mathrm{p}}} \tag{3.28}$$

where $\partial H/\partial T$ is the heat storage capacity of the moist building material (J/kg), $\partial w/\partial \phi$ is the moisture storage capacity (kg/m^3 %), w is the moisture content (kg/m^3), λ is the thermal conductivity (W/m K), D_{ϕ} is the liquid conduction coefficient (kg/ms), δ_p is the water vapour permeability (kg/ms Pa), h_v is the evaporation enthalpy of the water (J/kg), p_{sat} is the water vapour saturation pressure (Pa), T is the temperature (K), ϕ is the relative humidity (%), μ is the vapour diffusion resistance factor (−), δ_a is the vapour permeability in air (kg/ms Pa) and P_n is the normal atmospheric pressure (Pa).

3.15 Summary

The programs available for the public in general were analysed in detail (see Table 3.2), namely the input of material properties and the boundary conditions (inside and outside). In Table 3.2 we present all the physical parameters needed to

the hygrothermal modelling tools presented above. The most important exterior environmental loads (influence directly the transport of moisture) are:

- Ambient temperature;
- Ambient relative humidity;
- Solar diffuse;
- Solar direct;
- Cloud index;
- Wind velocity;
- Wind orientation;
- Horizontal rain precipitation.

Finally, as the purpose of most hygrothermal models is usually to provide sufficient and appropriate information needed for decision-making, we suggested four items that should be used when modelling a single component of the building envelope or a multizonal building:

- The software must be in the public domain (freeware or commercially) available;
- Suitability of the software for the single component or a multizonal building analyse under consideration;
- The programs must be of reasonably recent vintage or with recent further development;
- The software must be "user friendly".

List of symbols

(1) Bulk density
(2) Porosity
(3) Specific heat capacity
(4) Thermal conductivity
(5) Sorption isotherm
(6) Vapour permeability
(7) Vapour diffusivity
(8) Suction pressure
(9) Liquid diffusivity
(10) Diffusion resistance factor
(11) Water conductivity
(12) Specific moisture capacity
(13) Air permeability
(14) Hysteresis in sorption isotherm

(A) Temperature
(B) Rel. humidity/dew point/vapour pressure/ concentration
(C) Air pressure
(D) Solar radiation
(E) Wind velocity
(F) Wind direction
(G) Precipitation
(H) Long-wave exchange
(I) Cloud index
(J) Water leakage

(a) Temperature
(b) Rel. humidity/dew point/ vapour pressure/ concentration
(c) Air pressure
(d) Interior stack effect

As the programs have different hygrothermal potentialities, strengths and weaknesses, such as the availability to modelling the heat and moisture transfer by air movement, 2-D or 3-D phenomena, or the capability to simulate high number of zones in a reasonable execution time; the investigators need to select the hygrothermal simulation tools that suits better to their problems.

In conclusion, all simulation tools should:

- Calculate correctly and be possible to validate;
- Enable efficient information input and verification;

- Be robust;
- Be adaptable to non-standard problem types;
- Be transparent (possible to understand underlying mathematical model);
- Provide easy result analysis.

However, some programs have several limitations. For example, the UMIDUS version only includes Brazilian climatic data and the weather data for other cities and countries cannot be generated. The MOIST model does not appear to be undergoing any further development and technical support is no longer provided. The GLASTA program is only appropriate to check condensation and to simulate drying and the EMPTIED model doesn't take into account the influence of wind, sun and rain. Finally, the MATCH model is the hygIRC version of the more complete program BSim.

References

Burch DM, Chi J (1997). MOIST: a PC program for predicting heat and moisture transfer in building envelopes, Release 3.0, NIST special publication 917

Canada Mortgage and Housing Corporation-CMHM (2003) Review of hygrothermal models for building envelope retrofit analysis. Research highlights, Technical series 03–128

Hagentoft CE, BlombergT (2000) 1D-HAM coupled heat, air and moisture transport in multi-layered wall structures—manual of version 2.0. Lund–Gothenburg Group for Computational Building Physics

Hens H (1996) Heat, air and moisture transfer in insulated envelope parts. Modelling, final report, vol. 1, part 1, international energy agency, IEA ANNEX 24, K.U.-Leuven

Karagiozis A (2001) Advanced hygrothermal modelling of building materials using moisture-expert 1.0. In: Proceedings of the 35th international particleboard/composite materials symposium, Pullman Washington

Kalagasidis AS (2004) HAM-tools: an integrated simulation tool for heat, air and moisture transfer analyses in building physics. Ph.D. Thesis, Chalmers University of Technology, Gothenburg

Kuenzel H (1995) Simultaneous heat and moisture transport in building components—one and two dimensional calculation using simple parameters. Ph.D. Thesis, IBP Verlag, Stuttgart

Kuenzel HM, Kiessl K (1997) Calculation of heat and moisture transfer in exposed building components. Int J Heat Mass Transf 40(1):159–167

Kurnitski J, Vuolle M (2000) Simultaneous calculation of heat, moisture and air transport in a modular simulation environment. In: Proceedings of the Estonian academy of sciences engineering, vol 6, p 25

Mendes N, Ridley I, Lamberts R, Philip PC, Budag K (1999) UMIDUS—a PC program for the prediction of heat and moisture transfer in porous buildings elements, vol 20(4), pp 2–8. Building Energy Simulation, Berkeley

Nicolai A, Grunewald J, Zhang JS (2007) Salztransport und Phasenumwandlung - Modellierung und numerische Lösung im Simulationsprogramm Delphin 5. Bauphysik 3:231–239

Physibel (2007). GLASTA diffusion—condensation—drying extended Glaser method. http://www.physibel.be/v0n2gl.htm. Accessed Oct 19 2007

Rode C (1990) Combined heat and moisture transfer in building constructions. Ph.D. Thesis, Technical University of Denmark, Thermal Insulation Laboratory

Rode C, Grau K (2004) Calculation tool for whole building hygrothermal analysis building simulation 2000. IEA Annex 41 meeting, Zurich

Rousseau J (1999) Envelope moisture performance through infiltration, exfiltration and diffusion-EMPTIED. CMHM Technical Series 99–123

Salonvaara MH, Karagiozis AN (1994) Moisture transport in building envelopes using an approximate factorization solution method. In: Proceedings of the second annual conference of the CFD society of Canada, Toronto

van Schijndel AWM (2005) Integrated heat, air and moisture modelling and simulation in HAMLab. IEA ECBCS Annex 41, working meeting, Trondheim

Chapter 4
Application Examples

Hygrothermal modelling offers a powerful tool for predicting heat and moisture transport through multi-layer building assemblies. In this Chapter examples of the applicability of hygrothermal advanced simulation tools are presented.

4.1 Interior Superficial Temperature on Façades

Interstitial condensation, originating undesired liquid water inside components, can lead to degradation of variable severity depending on the type of materials that are affected. This process depends on components characteristics and boundary conditions (interior and exterior).

Relevant standardization in the field of hygrothermal behaviour and energy performance is being developed by the International Organization for Standardization (ISO) and by the European Committee for Standardization (CEN), which established the technical committee CEN/TC 89—Thermal Performance of Buildings and Building Components. This committee aims to study heat and moisture transfer and its effect on buildings behaviour.

This case study intends to evaluate, for the problem of interstitial condensation in building components, what is the structure of standardization for the available numerical simulation and connected experimental determination of material properties (see Ramos et al. (2009)).

Figures 4.1 and 4.2 show a schematic representation of the façade under study and the internal and external boundary conditions used in this application, respectively.

The hygrothermal numerical simulation tool used, as example, in this case study was WUFI 5.0. The program allows for the calculation of the transient hygrothermal behaviour of multi-layer building components exposed to natural climate conditions (see Kuenzel and Kiessl (1997)). This program is a one-dimensional model for heat and moisture transport analysis of building envelope components,

J. M. P. Q. Delgado et al., *Hygrothermal Numerical Simulation Tools Applied to Building Physics*, SpringerBriefs in Computational Mechanics,
DOI: 10.1007/978-3-642-35003-0_4, © The Author(s) 2013

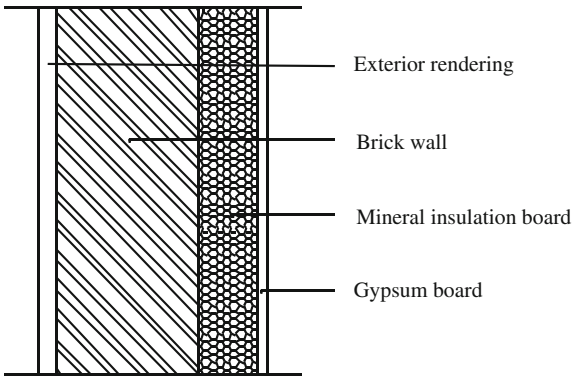

Fig. 4.1 Building component under study—exterior wall with interior insulation

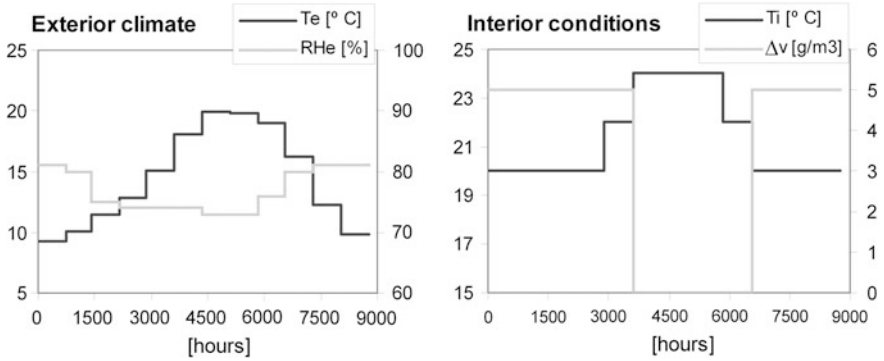

Fig. 4.2 Boundary condition for simulation

based on the finite volume method. The governing equations for moisture and energy transfer are represented by Eqs. (3.26) and (3.27), and the water vapour diffusion resistance factor, μ, used by the program is given by Eq. (3.28).

The model used by WUFI 5.0 is based on the standard EN 15026 (2007). It allows for a detailed knowledge of the hygrothermal state of the building component. It is possible to evaluate, for the simulation period, the hourly evolution of the component total moisture content. The variation of the moisture content, temperature and relative humidity for each layer or for a chosen location in the component is also available, not only through the simulation period, but also for the component profile for a specific point in time. Although its complexity, the model neglects:

(a) Convective transport (heat and moisture);
(b) Some of the liquid transport mechanisms, as seepage flow through gravitation, hydraulic flow through pressure differentials and electro-kinetic and osmotic effects;

(c) The interdependence of salt and water transport;
(d) The resistance of the interface between two capillary-active materials;
(e) The enthalpy flows resulting from the transport of liquid water due to temperature differential.

European standard EN 15026 (2007) provides minimum criteria for simulation software used to predict one-dimensional transient heat and moisture transfer in multi-layer building components exposed to transient climate conditions on both sides, and WUFI 5.0 complies with all requirements of this European standard. WUFI program requirements of material properties include: bulk density (kg/m^3), porosity (m^3/m^3), heat capacity (J/kg K), water content (kg/m^3) versus relative humidity, liquid transport coefficient (suction and redistribution) (m^2/s) versus water content (kg/m^3), heat conductivity (W/mK) versus water content (kg/m^3) and diffusion resistance factor versus relative humidity (%).

The application of WUFI 5.0 in the case study provides the variation with time of the moisture content in the building element and in each layer (see Fig. 4.3). It is also possible to know the moisture content profile at a given point in time (see Fig. 4.4).

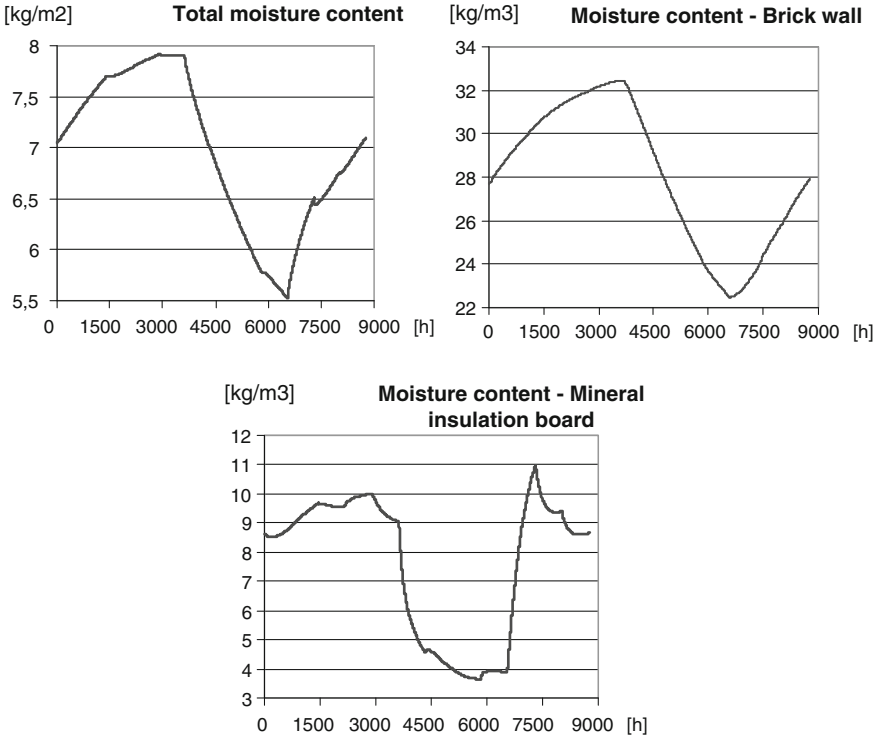

Fig. 4.3 Component moisture content variation over time

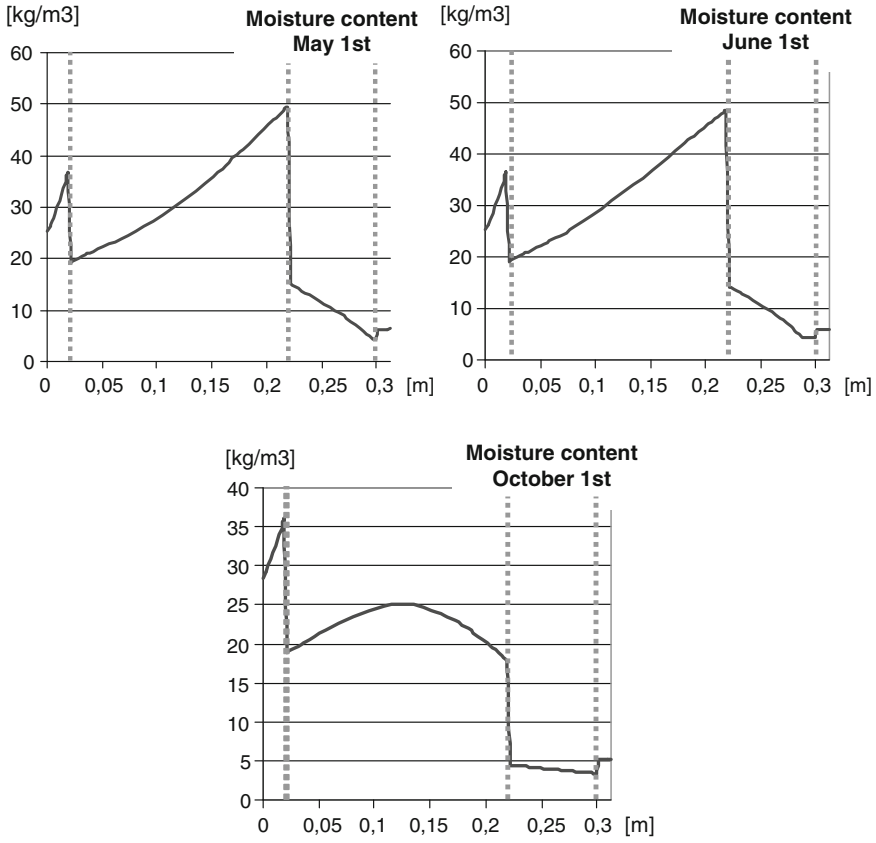

Fig. 4.4 Component moisture content profiles

The results obtained allow for extensive knowledge on each layer's moisture content development over time. This type of information is important for component optimization since it supports a detailed risk control strategy. As an example, it's possible to evaluate the increase of thermal conductivity of the mineral wool layer, due to the increase in moisture content during winter;

The hygrothermal tool indicated that, for the case study, interstitial condensation or the increase in moisture content would not cause severe damage, since the component would regain equilibrium during summer. But the more detailed simulation pointed out the decrease of insulating capacity during winter (see Fig. 4.5). This is due to the moisture content increase in mineral wool which implies an increase of thermal conductivity.

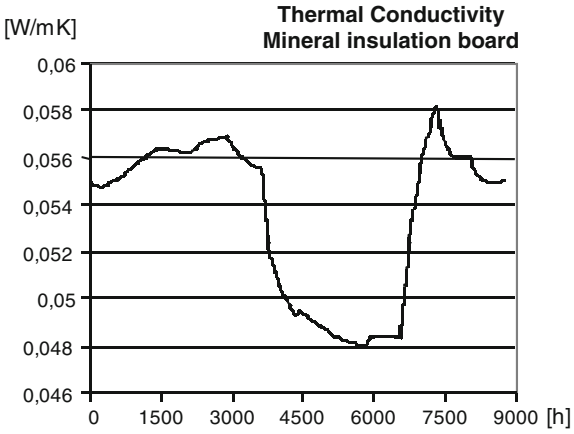

Fig. 4.5 Thermal conductivity variation over time

4.2 Water Content on Façades due to Wind-Driven Rain

The durability and hygrothermal performance of façades is highly influenced by wind-driven rain (WDR), once it is one of the major moisture sources for building façades (Blocken 2004). In a simple way, WDR is rain that is given a component by the wind that falls obliquely. It is characterized by a dynamic action (the impact of the rain drops) and by a static action (rain runoff on the façade).

The intent of this case study is to evaluate with a widely used numerical simulation program the influence of orientation, thickness of mineral plaster and short-wave radiation absorptivity of the exterior surface on the water content of a solid brick masonry when WDR is considered.

The hygrothermal numerical simulation tool used in this case study was WUFI 5.0. The governing equations for moisture and energy transfer are represented by Eqs. (3.26) and (3.27). The software supplies two semi-empirical models to calculate WDR: WUFI model and ASHRAE model. In this case study only ASHRAE model is used. The ASHRAE model can be found in ASHRAE 160 P (2009) where the WDR coefficient from Eq. 2.7, k, is calculated according to Eq. 4.1.

$$k = F_D \cdot F_E \cdot 0.2 \tag{4.1}$$

where k is the WDR coefficient (s/m), F_E is the rain exposure factor depending on the surrounding terrain and the height of the building (–) and F_D is the rain deposition factor which describes the building influence itself.

The values recommended for F_E and F_D are displayed in Tables 4.1 and 4.2.

Table 4.1 Rain deposition factor, F_D

Walls bellow a steed-slope roof	0.35
Walls bellow a low-slope roof	0.5
Walls subject to rain runoff	1

Table 4.2 Rain exposure factor, F_E

Height (m)	Type of terrain		
	Severe[a]	Medium	Sheltered[b]
<10	1.3	1.0	0.7
10–15	1.3	1.1	0.8
15–20	1.4	1.2	0.9
20–30	1.5	1.3	1.1
30–40	1.5	1.4	1.2
40–50	1.5	1.5	1.3
>50	1.5	1.5	1.5

[a] includes hilltops, coastal areas and funnelled wind
[b] includes shelter from trees, nearby buildings, or a valley

In the simulations a rain water absorption factor (r.r.f) or precipitation absorptivity was admitted. As it has not been fully studied it was used as an estimative the value 0.7. The WDR amount calculated by the semi-empirical models is then multiplied by the r.r.f.

It was studied a façade configuration consisting of a single-leaf wall of solid brick masonry (30 cm) with exterior mineral plaster and in the interior 5 cm of mineral wool and 1.5 mm of gypsum board (Fig. 4.1). The water content was calculated on an hourly basis over a period of five years. In the beginning all materials contain sorption moisture in equilibrium with an ambient humidity of 80 % relative humidity. The climatic data used was generated by Meteonorm (METEOTEST 2008) program for Porto. Meteonorm is a software tool that consists of a set of meteorological databases and a series of conversion utilities that prepare and format weather data for use with major hygrothermal modelling software packages. Meteonorm calculates hourly values of all parameters using a stochastic model and the resulting weather data files are produced in a variety of formats.

In Fig. 4.6 it can be seen how the orientation of the façade and the amount of WDR affect the water content of the masonry. The orientation with the highest driving rain load is not always the critical in terms of the water content of the masonry. The influence of solar radiation must also be evaluated as it influences the drying conditions. The moisture behavior of the wall is then determined by the balance between rain water absorption and the subsequent water release. The North direction is the one with the higher amount of water content and the South direction presents the minimum. This fact is due to the solar radiation (Fig. 4.7) because even though South has more WDR than North (Fig. 4.8) the solar radiation is much higher and so the drying process is faster. In these two orientations the solar radiation is the predominant factor.

The East façade shows higher water content values than West due to higher WDR load for East direction and the divergence of the temperature peak and the radiation peak (Fig. 4.9), which implies higher surface temperature on the West façade and lower water content of the masonry. From all façades, the one facing

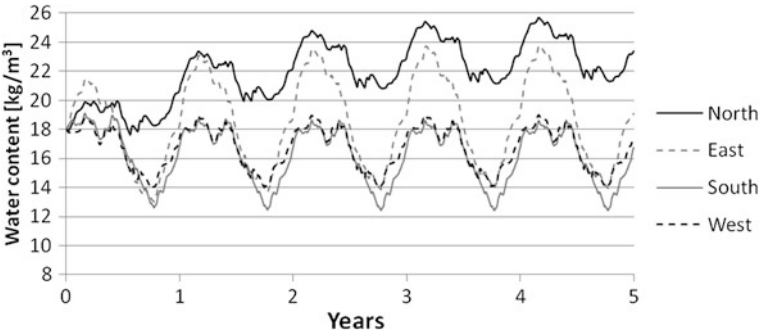

Fig. 4.6 Variation of water content on solid brick masonry with orientation (maximum WDR load)

Fig. 4.7 Annual amount of solar radiation for Porto

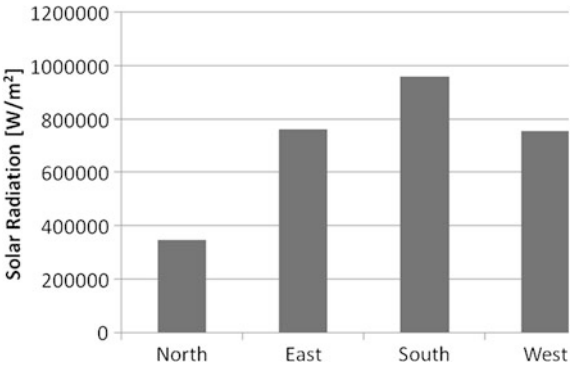

Fig. 4.8 Annual amount of WDR for Porto according to ASHRAE model

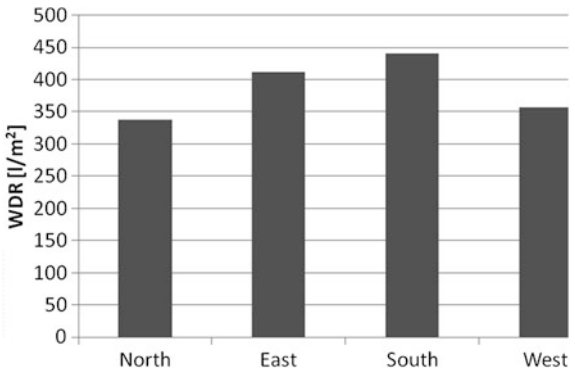

North is the only that presents an increase of water content along the years. The water content of the East façade clearly increases in the first 2 years and then stabilizes. The South and West façades maintain their maximum values of water

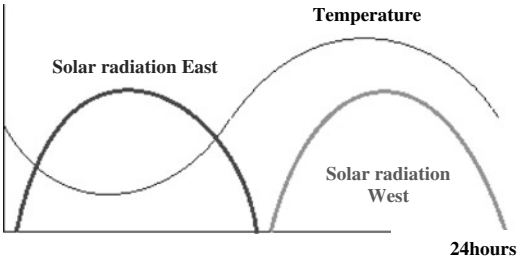

Fig. 4.9 Variation of solar radiation and temperature (24 h)

content along the years. For this load of WDR, the wall will not be able to dry out regardless orientation, although the North façade corresponds clearly to the worst scenario.

Considering a lower load of WDR, although the North façade still corresponds to the worst scenario and the South façade to the better one, the wall will, in this case, be able to dry out regardless orientation, as the water content decreases along the years (Fig. 4.10).

The thickness of the exterior mineral plaster also influences the water content of the brick wall. Figure 4.11 shows that when WDR load was reduced the thickness of this layer did not influenced the water content of the solid brick masonry. However when the WDR intensity increased the wall with 2 cm of exterior mineral plaster leaded to inferior values of water content comparing to the one with a rendering of 1.25 cm (reducing about 4 kg/m^3 in the year's maximum value).

The hygrothermal behaviour of the wall is also influenced by the characteristics of the stucco, such as the short-wave radiation absorptivity (α_s), which indicates the fraction of solar radiation incident on the component that is absorbed. In Figs. 4.12 and 4.13 it can be seen how α_s affects the water content in the

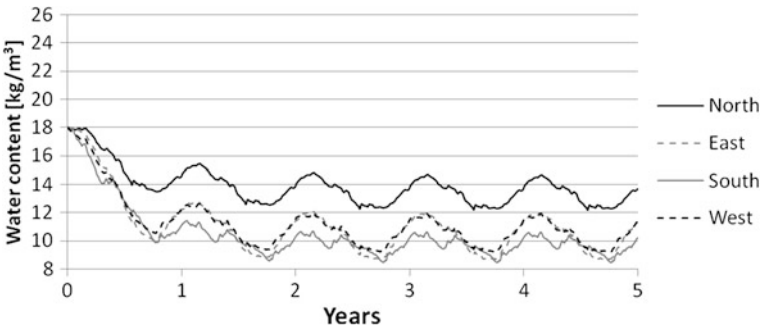

Fig. 4.10 Variation of water content on solid brick masonry with orientation (minimum WDR load)

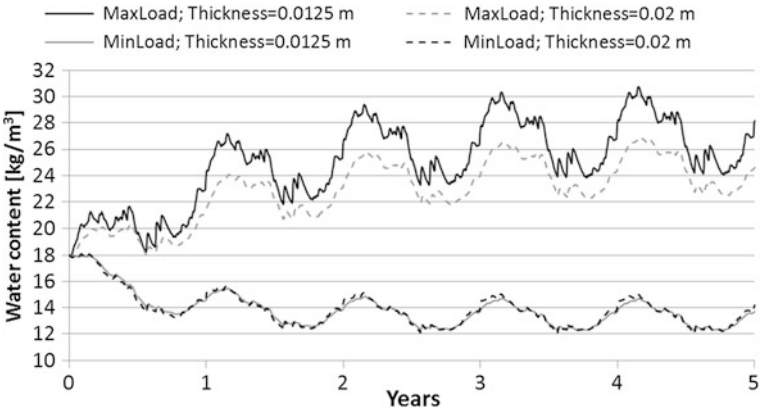

Fig. 4.11 Variation of water content on solid brick masonry for different mineral plaster thickness and WDR loads, for the North direction

masonry, considering the four cardinal directions and a bright ($\alpha_s = 0.2$) and a dark stucco ($\alpha_s = 0.6$).

It can be concluded that with $\alpha_s = 0.2$ the radiation absorbed is reduced what leads to lower surface temperatures and slower drying fluxes resulting in an increase of the water content in the masonry along the five years analysed. Since the influence of the radiation is reduced, in this case the East orientation has bigger water content peaks than the North because it also has higher loads of WDR. With an $\alpha_s = 0.6$ all the orientations show a stabilization or even a decrease in the water content and the North has bigger values of the water content because solar radiation regains its influence.

As a conclusion of this case study, it is possible to say that the water content varies with the orientation of the façade and in Porto the North façade, despite having the smallest amount of WDR has also the lower quantity of solar radiation and thus the drying potential is slower resulting in bigger water contents. On the

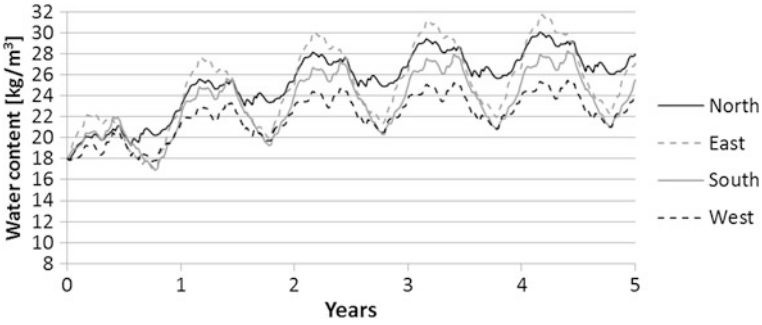

Fig. 4.12 Variation of water content on solid brick masonry with exterior mineral plaster with α_s = 0.2

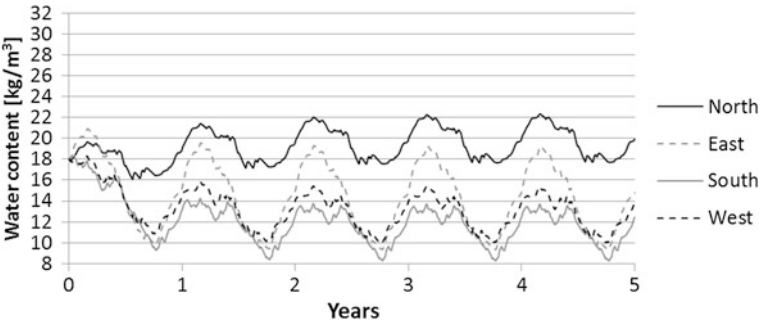

Fig. 4.13 Variation of water content on solid brick masonry with exterior mineral plaster with $\alpha_s = 0.6$

other hand, the South with the highest sum of solar radiation has the smaller water content for the façade. For the other directions it must be consider that the peak of temperature and radiation don't coincide for East and it results in lower superficial temperatures and in a slower drying flux and consequently in bigger water contents.

The effect of the exterior rendering thickness depends on the WDR intensity available for absorption. It was only for high amounts of WDR that the thickness changed the water content of the masonry (the bigger the thickness the better the hygrothermal behaviour).

The short-wave radiation absorptivity influences the balance of wetting and drying process. Lower values of α_s imply inferior surface temperatures and therefore an increase in the water content of the solid brick masonry. While stuccos with higher α_s result in smaller water contents.

4.3 Exterior Superficial Temperature on Façades

In this example it is presented the numerical results obtained with the hygrothermal softwares WUFI, HAM-Tools and hygIRC to evaluate the external surface temperature variations on external thermal insulation composite systems (ETICS) covering the west façade of a building located in Porto (Portuguese city). The knowledge of temperature and relative humidity conditions at the outer surface of walls are necessary for the study of condensations on façades, the undercooling phenomena.

The hygrothermal tools that can be used for assessing the undercooling phenomena are BSim, Delphin 5, HAMLab, HAM-Tools, hygIRC and WUFI. The 1D-HAM model just handle vapour diffusion and convection. Finally, the MOISTURE-EXPERT model has similar capabilities and potential applications of WUFI. The selection of the hygrothermal models, WUFI, HAM-Tools and

hygIRC, didn't respect any selection approach, only the fact that these three programs are the most used by the authors.

Figure 4.14 is a schematic of the test façade analysed numerically and Table 4.3 presents the material properties used in this application. The construction type chosen for comparison of the three hygrothermal models was a wall with external thermal insulation systems (ETICS) exposed to solar radiation.

The exterior and interior S_d value used was zero (no coating) and the interior heat transfer coefficient was constant and equal to 8 W/m^2 K. The exterior heat transfer coefficient only contained the convective part and was considered independent from the wind (constant value of 17 W/m^2 K).

All the calculations were done with climate data for Porto city obtained with METEONORM 6.0 (METEOTEST 2008). The weather data inputted to the models was temperature (°C), relative humidity (–), wind direction (°), wind speed (m/s), global solar radiation in a horizontal surface (W/m^2) and diffuse solar radiation in a horizontal surface (W/m^2). WUFI 5.0 also required information about air pressure (hPa), downward atmospheric radiation in a horizontal surface (W/m^2) and cloud index (two climatic file were created, one with downward atmospheric radiation and other with cloud index). HygIRC-1D also included information about the cloud index variation and HAM-Tools also demanded data about the air pressure (hPa) and the downward atmospheric radiation in a horizontal surface (W/m^2). In the climatic files rain was inputted equal to zero. The

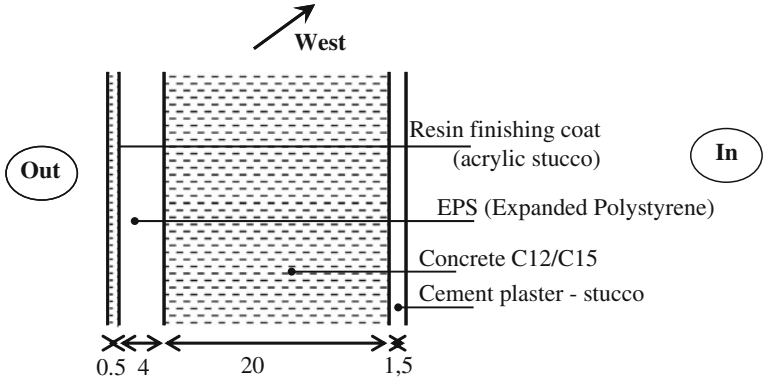

Fig. 4.14 Wall construction details (dimensions in cm)

Table 4.3 Material properties of wall components used in the hygrothermal models

Wall component	L (mm)	ρ_0 (kg/m^3)	ε (m^3/m^3)	λ (W/mK)	c_p (J/kgK)	μ (–)
Resin finishing coat (acrylic stucco)	5	2000	0.12	0.70	850	1000
EPS (Expanded polystyrene)	40	15	0.95	0.04	1500	30
Concrete	200	2200	0.18	1.6	850	92
Cement plaster—stucco	15	2000	0.30	1.20	850	25

conditions of indoor air were constant, with $RH = 60$ % and $T = 20$ °C (comfort values). The short wave radiation absorptivity and the long-wave radiation emissivity considered were 0.4 (stucco-normal bright) and 0.9, respectively, and the initial conditions within the element were $RH = 70$ % and $T = 15$ °C. The ground short-wave reflectivity was 0.2 and for WUFI 5.0 the ground long-wave emissivity was 0.9 and the ground long-wave reflectivity was 0.1.

The condensation on surface was assessed by comparing the surface temperature with the dew point temperature of outdoor air. Whenever the surface temperature drops below the dew point temperature condensations occur. The risk of condensation was evaluated by the monthly accumulated value of the positive differences between the dew point temperature of outdoor air and the surface temperature.

Regarding the treatment of the radiation effect on the exterior surface, all the three models use an explicit balance of the long-wave radiation, defining the surface emission, I_e, and the radiation arriving to it, I_l. They are combined with the shortwave radiation components into a collective heat source at the surface which may have positive or negative value, depending on the overall radiation balance: a positive value leads to heating up the component and a negative value leads to cooling it. With this methodology, the exterior heat transfer coefficient only contains the convective part.

$$q = \alpha_s \times I_s + \varepsilon_{l,surf} \times I_l - I_e \tag{4.2}$$

In Eq. (4.2), the two first items give the total amount of radiation (short and long) arriving to the surface, as according to Kirchoff Law the emissivity of a surface, $\varepsilon_{l,surf}$, is equal to its long-wave absorptivity. The last item is the radiation emitted by the building surface.

The total solar radiation, I_s, is described as a function of the direct solar radiation normal to component surface, $I_{s,dir}$, of the diffuse solar radiation, $I_{s,dif}$, affected by the atmospheric field of view, g_{atm}, and of the solar radiation reflected by the ground, $I_{s,ref}$, affected by the field of view of the ground, g_{ter}.

$$I_s = I_{s,dir} + g_{atm} \times I_{s,dif} + g_{ter} \times I_{s,ref} \tag{4.3}$$

The total long-wave radiation arriving to the surface, I_l, depends on the downward atmospheric radiation, $I_{l,atm}$, affected by the atmospheric field of view, g_{atm}.

$$I_l = g_{atm} \times I_{l,atm} \tag{4.4}$$

The sky radiation is ruled by the Plank Law, considering the concept of effective sky temperature, which can be defined as the temperature of a blackbody that emits the same amount of radiation as the sky (Martin and Berdahl 1984). The effective sky temperature depends on several atmospheric conditions, which are rarely available. For that reason, it is assumed that the sky behaves like a grey body, ruled by Stefan–Boltzmann Law, considering the sky emissivity and the air temperature near the ground (Finkenstein and Haupl 2007).

The downward atmospheric radiation in a specific location may be obtained through measurement, using pyrgeometers, or by empirical models (detailed methods are not commonly used because they require the knowledge of atmospheric conditions). According to Finkenstein and Haupl (2007), those empirical models provide satisfactory results for clear sky but the approaches for cloudy sky still point to very different results. The long-wave radiation emitted by the surface, I_e, depends on the surface emissivity, $\varepsilon_{l,surf}$, and temperature, T_{surf}, as it is ruled by the Stefan–Boltzmann Law.

$$I_e = \varepsilon_{l,surf} \times \sigma \times T_{surf}^4 \tag{4.5}$$

From the above equations, the direct solar radiation normal to component surface, $I_{s,dir}$, is automatically calculated by each model from the direct solar radiation in an horizontal surface, included in the climatic data, using information about the sun position. The diffuse solar radiation, $I_{s,dif}$ is obtained directly from the climatic data. The solar radiation reflected, $I_{s,ref}$, is calculated using solar radiation data (direct in an horizontal surface and diffuse) and the short wave radiation reflectivity of the ground.

The differences between the three models, regarding the heat exchange by radiation in the exterior surface, are related with the way the long-wave radiation emitted by the sky is obtained and the effect of the ground in the balance.

WUFI 5.0 allows two different approaches to obtain the atmospheric long-wave radiation, $I_{l,atm}$, necessary for the calculation: it may be read directly from the climatic file, if it has this information available, or it may be calculated using the cloud index data. This model also considers the emission and reflection of long-wave radiation by the ground, adding to Eq. (4.5) two extra items: the long-wave radiation emitted by the ground, calculated by the Stefan–Boltzmann Law assuming that the ground has the same temperature as the air and inputting the ground long-wave emissivity, and the atmospheric long-wave radiation reflected by the ground, calculated using the atmospheric long-wave radiation, $I_{l,atm}$, and the long-wave radiation reflectivity of the ground.

HygIRC-1D calculates the atmospheric long-wave radiation, $I_{l,atm}$, necessary for the simulation, using the cloud index information available in the climatic file. The effect of the ground (emission and reflection of long-wave radiation) is not taken into account.

HAM-Tools reads the atmospheric long-wave radiation, $I_{l,atm}$, necessary for the calculation directly from the climatic file. The effect of the ground (emission and reflection of long-wave radiation) is not included in the mathematical treatment.

The condensation on surface was assessed by comparing the surface temperature with the dew point temperature of outdoor air. Whenever the surface temperature drops below the dew point temperature condensations occur. The risk of condensation was evaluated using the concept of "accumulated degrees of condensation", which was calculated by accumulating during a certain period of time

(each month of the year under study) the hourly positive differences between the dew point temperature of outdoor air and the surface temperature. The negative differences were considered equal to zero.

$$\text{Accum.Degrees Cond.}_{\text{month}} = \sum \left(T_{\text{dp hourly}} - T_{\text{surface hourly}} > 0 \right) \tag{4.6}$$

The concept of "accumulated degrees of condensation" was necessary to evaluate the risk of condensation as the amount of accumulated condensate water on the surface is not a direct output some hygrothermal models.

In this case study simulations were done with three hygrothermal models to analyse the influence of the numerical treatment of the radiative balance in the exterior surface temperature of the wall in Fig. 4.14. It was possible to obtain similar temperatures on surface using all the models. The existing differences may be related with the calculations of the solar radiation normal to the surface that influences mostly the surface temperature during the day, but also after the sunset and at dawn. The differences can also be related with the formulation used to calculate the radiation emitted by the sky (WUFI 5.0_a and HAM-Tools use downward atmospheric radiation in a horizontal surface calculated by meteorological software and WUFI 5.0_b and HygIRC-1D calculate themselves the radiation using cloud index information). Differences in the governing equations and the conversion of the material properties may also have some effects on surface temperatures.

Figure 4.15 shows the variation in time of the calculated surface temperatures during a winter day (23rd of January) and Fig. 4.16 shows the accumulated degrees of condensation (or the sum of the positive differences between dew point temperature and the surface temperature) for the same day. It is possible to see that surface temperature drops below dew point temperature during the early morning

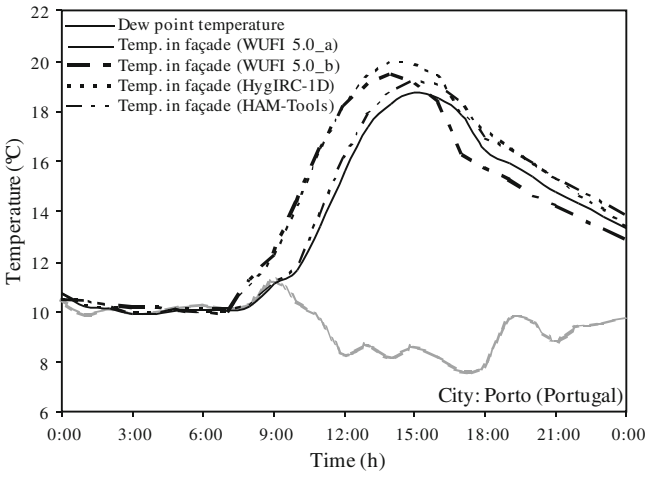

Fig. 4.15 Surface temperatures obtained by each hygrothermal model for Porto (23-January)

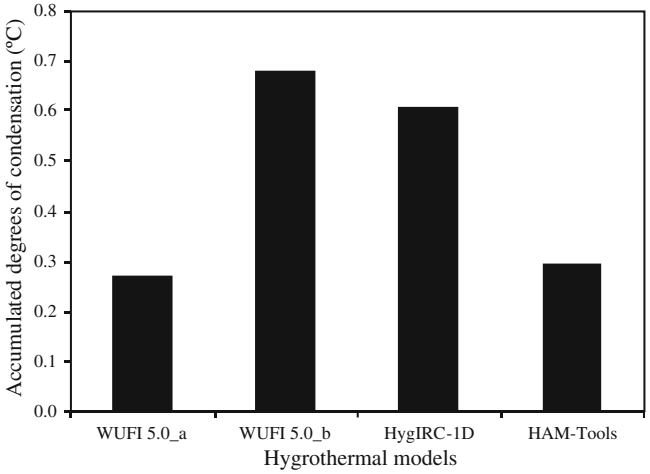

Fig. 4.16 Sum of positive differences between T_{dp} and T_{surf} for Porto (23-January)

hours for all models, due to the low thermal capacity of the system that allows the dissipation of the heat stored during the day in a few hours after sunset. Condensation occurs during this period of time.

There is however small differences between the models that induce the results presented in Fig. 4.16. Comparing WUFI 5.0_a and WUFI 5.0_b, of which only difference is the long-wave radiation used (in WUFI 5.0_a the radiation used was calculated by meteorological software and in WUFI 5.0_a was calculated by the equations included in the model using cloud index information), it shows that the values inputted for the long-wave radiation influence considerably the surface temperature and consequently the surface condensation. Figure 4.17 shows that the model used to calculate the atmospheric radiation induces significant differences in the obtained values. This is related with the difficulty in modelling atmospheric radiation with cloudy sky, referred previously. As radiation used in WUFI 5.0_a is higher than the one used in WUFI 5.0_b, surface temperatures are also higher and condensation reduce.

WUFI 5.0_b and HygIRC-1D present very similar variation of the surface temperature, especially during the night. This points to the similarity of the models, not only in term of governing equations but also in terms of boundary conditions. The effect of the ground included in WUFI 5.0_a may not have much influence in the phenomenon or it may compensate some differences existing between the two models. The similar values obtained for the surface temperature are also shown in Fig. 4.16, where the condensation values are also similar. WUFI 5.0_a and HAM-Tools both use the atmospheric radiation calculated by the meteorological software and their results are quite similar. The considerations made previously for WUFI 5.0_b and HygIRC-1D can also be applied to this case.

Figure 4.18 displays monthly accumulated degrees of condensation. The results show that the most pronounced condensations occur during the late summer, fall

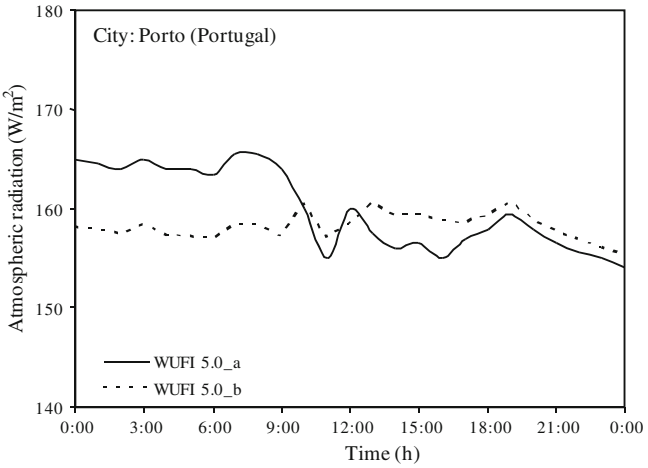

Fig. 4.17 Atmospheric radiation in a vertical plane in Porto (23-January)

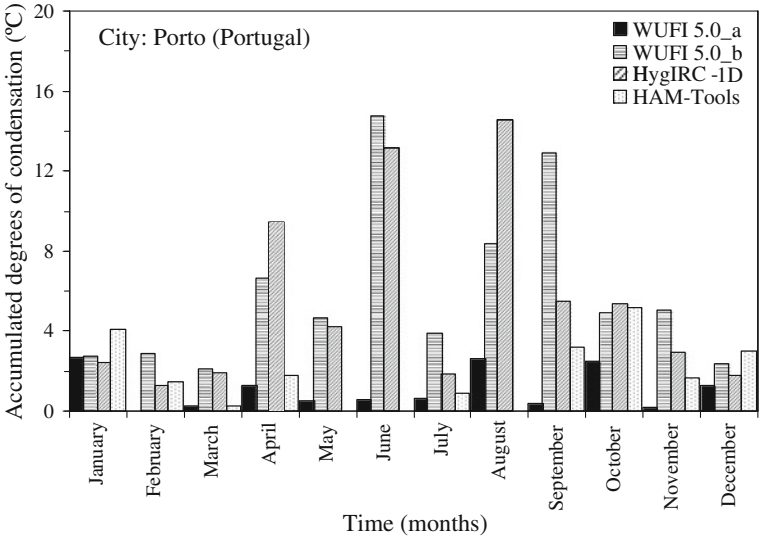

Fig. 4.18 Sum of positive differences between T_{dp} and T_{surf} for Porto

and winter months. This is related with the climatic conditions in Porto, a coastal town, namely its high relative humidity and mild temperatures all year-round. However, it should be remarked, once more, that the effect of long-wave radiation is quite clear, as WUFI 5.0_a and HAM-Tools have similar results and WUFI 5.0_b and HygIRC-1D also have similar results, but these two groups don't mach. In fact, the last two (WUFI 5.0_b and HygIRC-1D) have quite higher condensation as radiation is lower.

Figure 4.18 also shows that there are very few accumulated degrees of condensation in every month, using any program, and this is due to the small differences between the dew point temperature and the surface temperature, which are, on average, around 0.2 °C per hour. On the other hand, condensation occurs, on average, only half an hour per day during the year.

This application shows hygrothermal behaviour of an ETICS system. This kind of numerical results are very helpful to solve different problems in real life (for example: the algae growth on façades).

References

ASHRAE, 160P (2009) Criteria for moisture control design analysis in buildings. ASHRAE, USA

Blocken B (2004) Wind-driven rain on buildings—measurements, numerical modelling and applications. Ph.D. thesis, Katholieke Universiteit Leuven, Leuven

EN 15026 (2007) Hygrothermal performance of building components and elements—assessment of moisture transfer by numerical simulation. British Standards, London, UK

Finkenstein C, Haupl P (2007) Atmospheric long wave radiation being a climatic boundary condition in hygrothermal building part simulation. In: Proceedings of the 12th symposium for building physics, vol 2, Technische Universitat Dresden, Germany, pp 617–624

Kuenzel HM, Kiessl K (1997) Calculation of heat and moisture transfer in exposed building components. Int J Heat Mass Transf 40(1):159–167

Martin M, Berdahl P (1984) Summary of results from the spectral and angular sky radiation measurement program. Solar Energy 33(3–4):241–252

METEOTEST (2008) Meteonorm—Version 6.0. Meteotest, Bern, Switzerland

Ramos NMM, Delgado JMPQ, Barreira E, Freitas VP (2009) Hygrothermal properties applied in numerical simulation: interstitial condensation analysis. J Build Appr 5(2):161–170

Chapter 5
Conclusions and Perspectives

This brief review of heat, air, and moisture (HAM) analysis methods commonly used in numerical simulation is the major outcome of this work. The review has shown that there are numerous hygrothermal models with a range of capabilities and that these models are important tools to better understand the real problems and to provide correct solutions.

Hygrothermal simulation can be implemented with different complexity degrees. An important difference between models is the ability to tackle transient behaviour, since steady state conditions will frequently be a rough approximation to reality. Standardization also supports hygrothermal simulation contributing to higher feasibility of model application by designers.

A case study of interstitial condensation risk assessment allowed showing the importance of the advanced models as support for component optimization. The hygrothermal advanced models are more demanding regarding user ability to interpret results and material data availability. If a designer is defining, for instance, a solution for improving the thermal resistance of an existing building element he must therefore decide which type of modelling should be applied to solve a specific problem. A possible approach could be to start with the simpler model and evaluate if the intended solution has any risk of interstitial condensation. This first approach should be developed on the safe side, using worst case scenario boundary conditions. If risk of condensation is detected and cost optimization is relevant, more complex modelling can be produced, allowing, for instance, for a suitable design of a vapour barrier.

In the second case study it was shown how hygrothermal models allow simulating the behaviour of a building component considering the effect of WDR. WDR is directly calculated by the software tools using semi-empirical models that estimate the amount of rain that reaches the façade, based on the weather data for normal rain, wind velocity and wind direction. It was assessed the influence of orientation of the façade and thickness and short-wave radiation absorptivity of the exterior rendering on the water content of a solid brick masonry when WDR is

J. M. P. Q. Delgado et al., *Hygrothermal Numerical Simulation Tools Applied to Building Physics*, SpringerBriefs in Computational Mechanics,
DOI: 10.1007/978-3-642-35003-0_5, © The Author(s) 2013

considered. Orientation affects the water content of the wall not only because it changes the WDR loads but also because the effect of direct solar radiation differs considerably for different directions, which influences the drying fluxes. The effect of the exterior rendering thickness is only significant on the water content of the masonry when the WDR intensity available for absorption is higher. Otherwise it has almost no influence. The short-wave radiation absorptivity influences the balance of wetting and drying process and consequently the water content of the masonry wall.

In the third case study, the numerical results show that these programs are useful tools to simulate the undercooling phenomenon and assessing the exterior condensation on façades, providing that all relevant components of radiation exchange at the exterior surface are included in calculations. The models present similar results except when different inputs of long-wave radiation are used. In fact, it seems to be the key factor for the differences observed in the calculated values. Using cloud index information or measured long-wave radiation, even in the same model, provided the most significant differences.

Using accumulated degrees of condensation, a comparative measure of the risk of condensation on exterior surfaces can be obtained. Since very small differences between surface and dew point temperature contribute to this indicator, the calculations are therefore demanding in terms of required precision.

As described above, the models and simulation tools are able to represent the HAM behaviour of buildings at different levels of complexity. However, more validation cases are needed, possibly as a comparison with measurement data, experiences from practice and field tests. Moreover, with the objective to consolidate the knowledge this validation should be complemented with extensive sensitivity studies.